Output-feedback control for stabilization on SE(3)

Rita Cunha [a,*] , Carlos Silvestre [a] , João Hespanha [b]

[a] *Department of Electrical Engineering and Computer Science, Institute for Systems and Robotics, Instituto Superior Técnico, 1046-001 Lisbon, Portugal.*

[b] *Department of Electrical and Computer Engineering, University of California, Santa Barbara, CA 93106-9560, USA.*

Abstract

This paper addresses the problem of stabilizing systems that evolve on SE(3). The proposed solution consists of an output-feedback controller that guarantees almost global asymptotic stability of the desired equilibrium point, in the sense that the equilibrium point is stable and we have convergence for all initial conditions except for those in a nowhere dense set of measure zero. The output vector is formed by the position coordinates, expressed in the body frame, of a collection of landmarks fixed in the environment. The resulting closed-loop system exhibits the following properties: *i)* the position and orientation subsystems are decoupled, *ii)* the position error is globally exponentially stable, and *iii)* the orientation error is almost globally exponentially stable. Results are also provided that allow one to select landmark configurations so as to control how the position and orientation of the rigid body converge to their final equilibrium values.

Key words: Stabilization; Nonlinear Systems; Output-feedback; Rigid body stabilization

1. Introduction

The classical approach to the stabilization in position and orientation of a fully actuated rigid body relies on a local parameterization of the rotation matrix, such as the Euler angles, which transforms the state-space into an Euclidean vector space [19]. In this setting, the problem admits a trivial solution. However, no global solution can be obtained and there is no guarantee that the generated trajectories will not lead the system to one of its geometric singularities. Moreover, the described trajectories may be practically inadequate, since the norm of the Euler angles vector does not correspond to a metric on the Special Orthogonal Group SO(3) [16]. An alternative way of parameterizing rotations, which still has ambiguities but is globally nonsingular, is offered by the unit quaternions. Several examples in the literature address the problem of spacecraft attitude control using quartenion based solutions [21,15,12,9]. For example, Isidori et al. [9] present a nonlinear controller based on quaternions that solves an attitude regulation problem for low-Earth orbit rigid satellites. This and other param-

* Corresponding author. Tel.: +351-21-8418090; fax: +351-21-8418291.
Email address: rita@isr.ist.utl.pt (Rita Cunha).

eterizations are also applied in different settings, such as in [14], where Malis and Chaumette use the angle-axis representation to tackle a visual-servoing problem. However, all these examples require full state knowledge and special care to avoid discontinuities when mapping the current orientation to the selected parameter representation.

In this paper, we present an output-feedback solution to the problem of rigid-body stabilization, defined on a setup of practical significance. It is assumed that there is a collection of landmarks fixed in the environment and that the coordinates of the landmarks' positions are provided to the system. The proposed solution assumes that these coordinates are expressed in the body frame and therefore match the type of measurements produced by a number of on-board sensors. Examples of such sensors include CCD cameras, laser scanners, pseudo-GPS, etc.

The main contribution of this paper is the design of an output-feedback control law, based on the described measurements, that guarantees almost GAS of the desired equilibrium point. In loose terms, this corresponds to saying that the point is stable and that the solution converges asymptotically to that point, except for a nowhere dense zero measure set of initial conditions [2,5]. The relaxation in the notion of GAS from global to almost global provides a suitable framework for the stability analysis of systems evolving on manifolds not diffeomorphic to an Euclidean vector space, as is the case of the Special Euclidean Group SE(3) [16]. As discussed in [3,11,1,13], topological obstacles preclude the possibility of globally stabilizing these systems by means of continuous state feedback.

The approach followed in this paper is in line with the methods presented in [11,4,6], which address the attitude tracking problem on SO(3) based on the so-called modified trace function. Building on these results, we address the more general problem of stabilization in SE(3) and, equally important, we provide a controller that only requires output feedback, as opposed to full-state.

The proposed control law decouples the position and orientation subsystems and guarantees global exponential stability (GES) of the position error and almost GES of the orientation error. In addition, we establish results that describe the effect of the geometry of the points on the dynamic behavior of the closed-loop system. In particular, we show that the absolute value of the angle in an angle-axis parameterization of the rotation matrix decreases monotonically to zero. Moreover, the axis of rotation can be made almost GAS by appropriate landmark placement. Notice that while it suffices that the angle of rotation goes to zero for the rotation matrix to converge to the identity matrix, the convergence of the axis of rotation to an equilibrium provides further insight on how the rigid body moves to the final configuration.

The paper is organized as follows. Section 2 introduces the problem of stabilization on SE(3) and defines the output vector considered. Section 3 describes the construction of an almost globally asymptotically stabilizing state feedback controller for the system at hand. In the process, an exact expression for the region of attraction is derived. In Section 3.1, we show that the proposed control law can be expressed solely in terms of the output, and then analyze the convergence of the position and orientation errors and of the angle and axis of rotation arising from the angle-axis parameterization of the error rotation matrix. Section 3.2 extends the preceding results to address the problem of tracking a moving reference. Simulation results that illustrate the performance of the control system are presented in Section 4. Section 5 summarizes the contents of the paper and presents directions for future work. A preliminary version of a subset of these results was presented at the Conference on Decision and Control and can be found in

[8].

2. Problem formulation

Consider a fully actuated rigid body, attached to a frame $\{B\}$ and whose kinematic model is described by

$$\dot{\mathbf{p}} = \mathbf{v} - S(\boldsymbol{\omega})\mathbf{p} \tag{1a}$$

$$\dot{R} = RS(\boldsymbol{\omega}), \tag{1b}$$

where $\mathbf{p} \in \mathbb{R}^3$ is the position of the rigid body with respect to a fixed frame $\{I\}$, expressed in $\{B\}$, $R \in \mathrm{SO}(3)$ is the rotation matrix from $\{I\}$ to $\{B\}$, $\mathbf{v}$, $\boldsymbol{\omega} \in \mathbb{R}^3$ are the linear and angular velocities of $\{B\}$ with respect to $\{I\}$, expressed in $\{B\}$, and $S(.)$ is a function from $\mathbb{R}^3$ to the space of three by three skew-symmetric matrices $\mathrm{so}(3) = \{M \in \mathbb{R}^{3\times 3} : M = -M^T\}$ defined by

$$S\left(\begin{bmatrix} a_1 \\ a_2 \\ a_3 \end{bmatrix}\right) = \begin{bmatrix} 0 & -a_3 & a_2 \\ a_3 & 0 & -a_1 \\ -a_2 & a_1 & 0 \end{bmatrix}. \tag{2}$$

Note that S is a bijection and verifies $S(\mathbf{a})\mathbf{b} = \mathbf{a} \times \mathbf{b}$, where $\mathbf{a}, \mathbf{b} \in \mathbb{R}^3$ and $\times$ is the vector cross product.

Defining $(\mathbf{p}, R) \in \mathrm{SE}(3)$ as the configuration of $\{B\}$ with respect to $\{I\}$, consider also the desired target configuration $(\mathbf{p}^*, R^*) \in \mathrm{SE}(3)$ defined as the configuration of the desired body frame $\{D\}$ (assumed to be fixed in the workspace) with respect to $\{I\}$. In loose terms, the control objective consists of designing a control law for $\mathbf{v}$ and $\boldsymbol{\omega}$ that ensures the convergence of $(\mathbf{p}, R)$ to $(\mathbf{p}^*, R^*)$ (or, equivalently, of $\{B\}$ to $\{D\}$), with the largest possible basin of attraction. This control law uses measurements that come in the form of the coordinates of n fixed landmarks expressed in the body frame. The coordinates of these points, which we call landmarks, are available both in the current body frame $(\mathbf{p}, R)$ and in the desired body frame $(\mathbf{p}^*, R^*)$, as shown in Figure 1. This type of measurements are typically produced by on-board sensors that are able to locate landmarks fixed in the environment. Because the sensors are on-board, they produce the coordinates of the landmarks positions in the body frame. Examples of such sensors include CCD cameras, ladars, pseudo-GPS, etc.

Fig. 1. Problem setup.

According to Figure 1, we define the matrix of inertial landmark coordinates

$$X = [\mathbf{x}_1 \ \dots \ \mathbf{x}_n] \in \mathbb{R}^{3\times n}, \tag{3}$$

where $\mathbf{x}_j \in \mathbb{R}^3$ denotes the coordinates of the jth point expressed in $\{I\}$, and the matrix of body landmark coordinates

$$Q = [\mathbf{q}_1 \ \dots \ \mathbf{q}_n] \in \mathbb{R}^{3\times n}, \tag{4}$$

where

$$\mathbf{q}_j = R\mathbf{x}_j - \mathbf{p}, \quad j \in \{1, 2, \dots, n\}, \tag{5}$$

denotes the coordinates of the jth point expressed in $\{B\}$. Similarly, we introduce the target matrix $Q^* = [\mathbf{q}_1^* \ \dots \ \mathbf{q}_n^*] \in \mathbb{R}^{3\times n}$, where $\mathbf{q}_j^* = R^*\mathbf{x}_j - \mathbf{p}^*$. Defining the vector $\mathbf{1} = [1 \cdots 1]^T \in \mathbb{R}^n$, Q and Q^* can be rewritten as

$$Q = RX - \mathbf{p}\mathbf{1}^T, \quad Q^* = R^*X - \mathbf{p}^*\mathbf{1}^T,$$

respectively. The landmarks are required to satisfy the following conditions:

Assumption 1 *At least three of the $n \geq 3$ points are not collinear.*

Assumption 2 *The origin of $\{I\}$ belongs to the interior of the landmarks' convex hull.*

Using (3), it is straightforward to observe that Assumption 2 is equivalent to the set of algebraic conditions specified in the following proposition.

Proposition 3 *Assumption 2 is satisfied if and only if there exists a vector $\mathbf{a} = [a_1 \dots a_n]^T \in \mathbb{R}^n$ such that $X\mathbf{a} = 0$, $\mathbf{1}^T\mathbf{a} = 1$, and $a_j > 0$, $j \in \{1, 2, \dots, n\}$.*

To conclude the problem formulation, we introduce the error variables

$$\mathbf{e} = \mathbf{p} - \mathbf{p}^* \in \mathbb{R}^3, \quad R_e = R^* R^T \in \mathrm{SO}(3), \tag{6}$$

and the state-space model for the error system, which can be written as

$$\dot{\mathbf{e}} = \mathbf{v} - S(\boldsymbol{\omega})(\mathbf{e} + \mathbf{p}^*) \tag{7a}$$

$$\dot{R}_e = -S(R^*\boldsymbol{\omega})R_e, \tag{7b}$$

with the output vector given by (4). The control objective can then be defined as that of designing a control law based on Q that drives $\mathbf{e}$ to zero and R_e to the identity matrix I_3.

3. Control design on SE(3)

The approach adopted to solve the proposed stabilization problem builds on Lyapunov theory and, for that purpose, the following candidate Lyapunov function is considered

$$V = \frac{1}{2}\mathrm{tr}((Q - Q^*)D_a(Q - Q^*)^T) \tag{8}$$

where

$$D_a = \mathrm{diag}(\mathbf{a}) \in \mathbb{R}^{n \times n} \tag{9}$$

and $\mathbf{a} = [a_1 \dots a_n]^T \in \mathbb{R}^n$ is the vector defined in Proposition 3 such that $X\mathbf{a} = 0$, $\mathbf{1}^T\mathbf{a} = 1$, and $D_a > 0$.

Since we are concerned with the global asymptotic stabilization of a system evolving on SE(3), it is convenient to express V as a function on SE(3). With that objective in mind, we introduce the constant matrices

$$M = XD_aX^T \in \mathbb{R}^{3\times 3}, \tag{10}$$

$$P = \mathrm{tr}(M)I_3 - M \in \mathbb{R}^{3\times 3}, \tag{11}$$

and describe some of their properties, which will be useful for the forthcoming derivations.

Proposition 4 *The matrices M and P can be rewritten as*

$$M = \sum_{j=1}^{n} a_j \mathbf{x}_j \mathbf{x}_j^T \tag{12}$$

$$P = -\sum_{j=1}^{n} a_j S(\mathbf{x}_j)^2. \tag{13}$$

Moreover, when Assumptions 1 and 2 hold, P is positive definite.

PROOF. The matrix M given in (10) can be rewritten as

$$M = XD_aX^T = \begin{bmatrix}\mathbf{x}_1 & \cdots & \mathbf{x}_n\end{bmatrix} \begin{bmatrix} a_1\mathbf{x}_1^T \\ \vdots \\ a_n\mathbf{x}_n^T \end{bmatrix} = \sum a_j \mathbf{x}_j \mathbf{x}_j^T.$$

Then, it is easy to see that

$$\begin{aligned} P = \mathrm{tr}(M)I_3 - M &= (\textstyle\sum a_j \mathbf{x}_j^T \mathbf{x}_j)I_3 - \sum a_j \mathbf{x}_j \mathbf{x}_j^T \\ &= \textstyle\sum a_j(\mathbf{x}_j^T\mathbf{x}_j I_3 - \mathbf{x}_j\mathbf{x}_j^T) = -\sum a_j S(\mathbf{x}_j)^2. \end{aligned}$$

If Assumption 2 holds then $a_j > 0$ for $j \in \{1, 2, \dots, n\}$ and therefore

$$\mathbf{u}^T P \mathbf{u} = \textstyle\sum \mathbf{a}_j \|S(\mathbf{x}_j)\mathbf{u}\|^2 \geq 0, \quad \forall \mathbf{u} \in \mathbb{R}^3$$

and

$$\mathbf{u}^T P \mathbf{u} = 0 \Leftrightarrow S(\mathbf{x}_j)\mathbf{u} = 0, \forall j \in \{1, 2, \dots, n\}. \tag{14}$$

If Assumption 1 holds, (14) is verified if and only if $\mathbf{u} = 0$. □

To gain further insight, we also consider the angle-axis parameterization for orientation [16], according to which we can represent $R_e \in \mathrm{SO}(3)$ as a rotation of angle $\theta \in [0, \pi]$ about an axis $\mathbf{n} \in \mathbb{S}^2 \triangleq \{\mathbf{x} \in \mathbb{R}^3 : \mathbf{x}^T\mathbf{x} = 1\}$ using the map

$$\begin{aligned} &\mathrm{rot} : ([0, \pi], \mathbb{S}^2) \to \mathrm{SO}(3) \\ &\qquad (\theta, \mathbf{n}) \mapsto I_3 + \sin\theta S(\mathbf{n}) + (1 - \cos\theta)S(\mathbf{n})^2. \end{aligned} \tag{15}$$

Notice that the map rot(.,.) is surjective but not injective. For instance, $\text{rot}(0, \mathbf{n}) = I_3$ and $\text{rot}(\pi, \mathbf{n}) = \text{rot}(\pi, -\mathbf{n})$, for all $\mathbf{n} \in \mathbb{S}^2$. More details on the angle-axis parameterization can be found in Appendix A.

In what follows, all expressions are first derived as functions of $R_e \in \text{SO}(3)$ and only then written in terms of an angle $\theta \in [0, \pi]$ and an axis $\mathbf{n} \in \mathbb{S}^2$. Consequently, they are independent of the parameterization and not affected by singularity problems. The angle-axis parameterization is used solely to help in interpreting the system's behavior and finding useful properties, such as the positive definiteness of a function.

The following Lemma shows how we can rewrite (8) as a function of $\mathbf{e}$ and R_e and verify that $V = 0$ if and only if $\mathbf{e} = 0$ and $R_e = I_3$.

Lemma 5 *Under Assumption 2, the candidate Lyapunov function V defined in* (8) *can be expressed as a function on* SE(3) *of the form*

$$V(\mathbf{e}, R_e) = V_1(\mathbf{e}) + V_2(R_e), \tag{16}$$

where

$$V_1(\mathbf{e}) = \frac{1}{2}\mathbf{e}^T\mathbf{e}, \tag{17}$$

$$V_2(R_e) = \text{tr}\left((I - R_e)M\right). \tag{18}$$

In addition, V_2 satisfies the following properties:

i) $V_2 \geq 0$, *for all* $R_e \in \text{SO}(3)$;

ii) when Assumption 1 holds, $V_2 = 0 \Leftrightarrow R_e = I_3$;

iii) for any $\theta \in [0, \pi]$ *and* $\mathbf{n} \in \mathbb{S}^2$ *such that* $R_e = \text{rot}(\theta, \mathbf{n})$, *$V_2$ can be written as*

$$V_2 = (1 - \cos\theta)\mathbf{n}^T P \mathbf{n}, \tag{19}$$

where P is given by (11).

PROOF. Recalling that $Q = RX - \mathbf{p}\mathbf{1}^T$ and $Q^* = R^*X - \mathbf{p}^*\mathbf{1}^T$, the expression for V given in (8) can be rewritten as

$$V = \tfrac{1}{2}\text{tr}\big([R^{*T}(R_e - I_3)X - \mathbf{e}\mathbf{1}^T]D_a \; [X^T(R_e^T - I_3)R^* - \mathbf{1}\mathbf{e}^T]\big).$$

Since under Assumption 2, we have $X\mathbf{a} = 0$, the cross terms $-R^{*T}(R_e - I_3)XD_a\mathbf{1}\mathbf{e}^T$ and its transpose are also equal to zero and we can write

$$\begin{aligned} V &= \tfrac{1}{2}\text{tr}(R^{*T}(R_e - I_3)M(R_e^T - I_3)R^*) + \tfrac{1}{2}\text{tr}(\mathbf{e}(\mathbf{1}^T\mathbf{a})\mathbf{e}^T) \\ &= \tfrac{1}{2}\mathbf{e}^T\mathbf{e} + \tfrac{1}{2}\text{tr}((R_e^T - I_3)(R_e - I_3)M) \\ &= V_1(\mathbf{e}) + V_2(R_e). \end{aligned}$$

Regarding *i)*, we can verify that $V_2 \geq 0$ by noting that, according to (12), V_2 can be rewritten as $V_2(R_e) = \frac{1}{2}\sum_j a_j \mathbf{x}_j^T(R_e^T - I_3)^T(R_e - I_3)\mathbf{x}_j$. Next, consider the claim in *iii)*. For any $\theta \in [0, \pi]$ and $\mathbf{n} \in \mathbb{S}^2$ such that $R_e = \text{rot}(\theta, \mathbf{n})$, we can use (15) to rewrite V_2 as

$$\begin{aligned} V_2 &= -\sin\theta\,\text{tr}(S(\mathbf{n})M) - (1 - \cos\theta)\text{tr}(S(\mathbf{n})^2M) \\ &= -\sin\theta\sum a_j\mathbf{x}_j^T S(\mathbf{n})\mathbf{x}_j + (1 - \cos\theta)\text{tr}((I_3 - \mathbf{n}\mathbf{n}^T)M) \\ &= (1 - \cos\theta)\mathbf{n}^T\left(\text{tr}(M)I_3 - M\right)\mathbf{n} \\ &= (1 - \cos\theta)\mathbf{n}^T P\mathbf{n} \end{aligned}$$

Finally, to prove *ii)*, notice that $V_2 = 0$ is equivalent to $\theta = 0$ if and only if $P > 0$ and, by Proposition 4, this is true if Assumptions 1 and 2 hold. □

The next step towards the definition of a control law based on V is that of determining an expression for $\dot{V} = \dot{V}_1 + \dot{V}_2$.

Lemma 6 *The time derivatives of V_1 and V_2 are given by*

$$\dot{V}_1 = \mathbf{e}^T(\mathbf{v} + S(\mathbf{p}^*)\boldsymbol{\omega}) \tag{20}$$

and

$$\dot{V}_2 = -S^{-T}(R_eM - MR_e^T)R^*\boldsymbol{\omega}, \tag{21}$$

respectively, where $S^{-1} : \text{so}(3) \mapsto \mathbb{R}^3$ corresponds to the inverse of the skew map S defined in (2). *In addition, for any $\theta \in [0, \pi]$ and $\mathbf{n} \in \mathbb{S}^2$ such that $R_e = \text{rot}(\theta, \mathbf{n})$,* (21) *can be written as*

$$\dot{V}_2 = -\mathbf{n}^T PN(\theta, \mathbf{n})^T R^*\boldsymbol{\omega}, \tag{22}$$

where $N(\theta, \mathbf{n}) = \sin\theta I_3 + (1 - \cos\theta)S(\mathbf{n})$.

PROOF. Differentiating V_1 and using (7a), we obtain

$$\begin{aligned}\dot{V}_1 &= \mathbf{e}^T\dot{\mathbf{e}} = \mathbf{e}^T(\mathbf{v} - S(\boldsymbol{\omega})(\mathbf{e}+\mathbf{p}^*))\\ &= \mathbf{e}^T(\mathbf{v} - S(\boldsymbol{\omega})\mathbf{p}^*).\end{aligned}$$

Taking the derivative of (18) and using (7b) and Proposition 20, we have

$$\begin{aligned}\dot{V}_2 &= -\mathrm{tr}(\dot{R}_e M) = \mathrm{tr}\left(S(R^*\boldsymbol{\omega})R_e M\right)\\ &= -S^{-\tau}(R_e M - M R_e^T)R^*\boldsymbol{\omega}.\end{aligned}$$

Let $\mathbf{a}$ be a vector in $\mathbb{R}^3$ and consider the angle-axis representation for R_e. Then, according to Proposition 20, we have

$$\begin{aligned}&\mathbf{a}^T S^{-1}(R_e M - M R_e^T) = -\mathrm{tr}\left(S(\mathbf{a})R_e M\right)\\ &= -\mathrm{tr}\left(S(\mathbf{a})(I_3 + \sin\theta\, S(\mathbf{n}) + (1-\cos\theta)(\mathbf{n}\mathbf{n}^T - I_3))M\right)\\ &= -\sin\theta\,\mathrm{tr}(S(\mathbf{a})S(\mathbf{n})M) - (1-\cos\theta)\,\mathrm{tr}(S(\mathbf{a})\mathbf{n}\mathbf{n}^T M)\\ &= -\sin\theta\,\mathrm{tr}\left((\mathbf{n}\,\mathbf{a}^T - \mathbf{a}^T\mathbf{n} I_3)M\right) - (1-\cos\theta)\,\mathbf{n}^T M S(\mathbf{a})\mathbf{n}\\ &= \sin\theta\,\mathbf{a}^T P\mathbf{n} + (1-\cos\theta)\,\mathbf{a}^T S(\mathbf{n})P\mathbf{n}\end{aligned}$$

and thus, $S^{-1}(R_e M - M R_e^T) = N(\theta,\mathbf{n})P\mathbf{n}$, where $N(\theta,\mathbf{n}) = \sin\theta\, I_3 + (1-\cos\theta)S(\mathbf{n})$. □

Before presenting a solution to the stabilization problem, we describe a preliminary approach to the problem that serves as motivation. According to Lemma 6, $\dot{V}$ can be written as

$$\dot{V} = \mathbf{a}_v^T\mathbf{v} + \mathbf{a}_\omega^T\boldsymbol{\omega}, \tag{23}$$

where $\mathbf{a}_v = \mathbf{e}$, $\mathbf{a}_\omega = -S(\mathbf{p}^*)\mathbf{e} - R^{*T}S^{-1}(R_e M - M R_e^T)$. In view of (23), the simplest state-feedback control law yielding $\dot{V} \leq 0$ would be

$$\mathbf{v} = -k_v\mathbf{a}_v,\ \boldsymbol{\omega} = -k_\omega\mathbf{a}_\omega, \tag{24}$$

with $k_v > 0$ and $k_\omega > 0$. This choice of controller guarantees, by Lyapunov's stability theorem, local stability of $(\mathbf{e}, R_e) = (0, I_3)$ and, by LaSalle's invariance principle, global convergence to the largest invariant set in the domain satisfying $\dot{V} = 0$. In this particular case, the whole set defined by $\dot{V} = 0$ is positively invariant, since all its elements are equilibrium points of the system. In summary, GAS would only be guaranteed if $(\mathbf{e}, R_e) = (0, I_3)$ were the unique solution of $\dot{V} = 0$. The following result discards this possibility.

Lemma 7 *Under Assumptions 1 and 2, the time derivative of V along the trajectories of the system* (7) *with the control law* (24) *is equal to zero if and only if $\mathbf{e} = 0$ and R_e belongs to the set*

$$\mathcal{C}_{V_2} = \{I_3\} \cup \{\mathrm{rot}(\pi,\mathbf{n}) \in \mathrm{SO}(3) : \mathbf{n} \textit{ is an eigenvector of } P\}. \tag{25}$$

PROOF. According to (23) and (24), we have

$$\dot{V} = 0 \Leftrightarrow \begin{cases}\mathbf{a}_v = 0\\ \mathbf{a}_\omega = 0\end{cases} \Leftrightarrow \begin{cases}\mathbf{e} = 0\\ S^{-1}(R_e M - M R_e^T) = 0\end{cases}$$

To solve $S^{-1}(R_e M - M R_e^T) = 0$ or, equivalently, $N(\theta,\mathbf{n})P\mathbf{n} = 0$, note that the null space of N is given by

$$\ker(N(\theta,\mathbf{n})) = \begin{cases}\mathbb{R}^3 & \text{if } \theta = 0\\ \mathrm{span}(\mathbf{n}) & \text{if } \theta = \pi\\ 0 & \text{otherwise}\end{cases},$$

and, since $P > 0$ and $\mathbf{n} \in \mathbb{S}^2$,

$$N(\theta,\mathbf{n})P\mathbf{n} = 0 \Leftrightarrow \theta = 0 \text{ or } \begin{cases}\theta = \pi\\ P\mathbf{n} \in \mathrm{span}(\mathbf{n})\end{cases}.$$

□

Since the matrix P is completely determined by the landmark positions that define X, Lemma 7 shows that C_{V_2} is determined by the geometry of the measured points. To illustrate this observation, consider two configurations for the landmark points, a rectangle and a square, corresponding to the matrices

$$X_1 = \begin{bmatrix}b & b & -b & -b\\ c & -c & -c & c\\ 0 & 0 & 0 & 0\end{bmatrix},\ X_2 = \begin{bmatrix}b & b & -b & -b\\ b & -b & -b & b\\ 0 & 0 & 0 & 0\end{bmatrix},$$

respectively, with $b > c > 0$. It is easy to see that the vector $\mathbf{a} = \frac{1}{n}\mathbf{1}$ satisfies $X_1\mathbf{a} = X_2\mathbf{a} = 0$ and $\mathbf{1}^T\mathbf{a} = 1$ and so $P_i = \frac{1}{n}(X_i X_i^T - \mathrm{tr}(X_i X_i^T)I_3)$, $i \in \{1,2\}$. Simple algebra shows

that, in the first case, $\dot{V}_2 = 0$ has exactly four solutions given by

$$C_{V_2}^{(1)} = \{I_3, \mathrm{diag}(-1,-1,1)\} \cup \{\mathrm{diag}(-1,1,-1), \mathrm{diag}(1,-1,-1)\}, \quad (26)$$

while, in the second, these solutions form the set

$$C_{V_2}^{(2)} = \{I_3, \mathrm{diag}(-1,-1,1)\} \cup \{R_e \in \mathrm{SO}(3) : R_e = \begin{bmatrix} \cos\psi & \sin\psi & 0 \\ \sin\psi & -\cos\psi & 0 \\ 0 & 0 & -1 \end{bmatrix}, \psi \in \mathbb{R}\}. \quad (27)$$

The sets $C_V^{(1)} = \{0\} \times C_{V_2}^{(1)}$ and $C_V^{(2)} = \{0\} \times C_{V_2}^{(2)}$ are depicted in Figures 2(a) and (b), respectively, where, for simplicity of representation, it is assumed that $R^* = I_3$ and $\mathbf{p}^* = [0\ 0\ d]^T$, $d > 0$. The desired configuration is represented in black by the vector $\mathbf{p}^*$ and the coordinate frame $\{D\}$. The remaining configurations are represented in gray. Lemma 7 reflects the topological obstacles, discussed in [3], [11], [1], and [13], to achieving, by continuous state feedback, global stabilization of systems evolving on manifolds not diffeomorphic to the Euclidean Space. In fact, given a system evolving on a manifold $\mathcal{M}$, GAS of a single equilibrium point would imply the existence of a smooth positive definite function $V : \mathcal{M} \mapsto \mathbb{R}$ with negative definite derivative over all $\mathcal{M}$, that could be viewed as a Morse function with a single critical point, and, to admit such a function, $\mathcal{M}$ would have to be diffeomorphic to the Euclidean Space [13]. In view of these obstacles, a relaxation in the notion of GAS from global to almost global needs to be considered. It allows for the existence of a nowhere dense zero measure set of initial conditions that do not tend to the specified equilibrium point. In practical terms, this relaxation is fairly innocuous, since disturbances or sensor noise will prevent trajectories from remaining at these (unstable) equilibria.

To formalize this notion of stability, which is adopted in [7], [17], and [2], we first recall the definition of region of attraction.

(a) rectangle - four solutions

(b) square - infinite number of solutions

Fig. 2. Set of configurations such that $\dot{V} = 0$ for two different landmark geometries.

Definition 8 (Region of Attraction) *Consider the following autonomous system evolving on a smooth manifold* $\mathcal{M}$

$$\dot{x} = f(x) \quad (28)$$

where $x \in \mathcal{M}$ *and* $f : \mathcal{M} \to T\mathcal{M} : x \mapsto f(x) \in T_x\mathcal{M}$ *is locally Lipschitz and suppose that* $x = x^*$ *is an asymptotically stable equilibrium point of the system. The region of attraction for* x^* *is defined as*

$$\mathcal{R}_A = \{x_0 \in \mathcal{M} : \phi(t, x_0) \text{ is defined for all } t \geq 0 \text{ and } \phi(t, x_0) \to x^* \text{ as } t \to \infty\} \quad (29)$$

where $\phi(t, x_0)$ denotes the solution to (28) *at time t, with initial condition $x(0) = x_0$.*

The reader is referred to [13] for the definition of a locally Lipschitz function defined on a manifold.

Definition 9 (Almost GAS) *Consider the system* (28)*. The equilibrium point $x = x^*$ is said to be almost globally asymptotically stable if it is stable and $\mathcal{M} \backslash \mathcal{R}_A$ is a nowhere dense set of measure zero.*

Going back to the original kinematic model (7), we define the following continuous feedback law based on the function V

$$\mathbf{v} = -k_v \mathbf{e} - k_\omega S(\mathbf{e} + \mathbf{p}^*)\mathbf{b}_\omega, \tag{30a}$$

$$\boldsymbol{\omega} = k_\omega \mathbf{b}_\omega, \tag{30b}$$

where

$$\mathbf{b}_\omega = R^{*T} S^{-1}(R_e M - M R_e^T),$$

This control law actually has the same equilibrium points as the simpler one considered before. However, we are now able to show that the desired equilibrium $(\mathbf{e}, R_e) = (0, I_3)$ is almost GAS, implying that the remaining equilibria are unstable and that their regions of attraction have at most zero measure. Additionally, we will see shortly that these control signals can be directly expressed in terms of the available measurements.

Theorem 10 *For any k_v and k_ω positive, the closed-loop system resulting from the interconnection of* (7) *and* (30) *has an almost GAS equilibrium point at $(\mathbf{e}, R_e) = (0, I_3)$. The corresponding region of attraction is given by*

$$\mathcal{R}_A = \mathrm{SE}(3) \setminus \{(\mathbf{e}, R_e) : \mathrm{tr}(I_3 - R_e) = 4\}. \tag{31}$$

Remark 11 *To prove almost GAS, we need to determine the actual region of attraction and not just an estimate of it, as could be readily obtained using Lyapunov's method. This would only provide us with a closed invariant set of the form $\Omega_c = \{x \in \mathcal{M} : V(x) \leq c\}$ that is guaranteed to be contained in the region of attraction $\mathcal{R}_A$ but that can never coincide with it, since $\mathcal{R}_A$ is necessarily an open set [10]. Instead, the proof of Theorem 10 relies on Zubov's theorem, which can be used to find the boundary of $\mathcal{R}_A$ (see [10] and [20]). For the sake of completeness, we restate the theorem, with only slight alterations with respect to the version presented in [20].* □

Theorem 12 (Zubov's Theorem) *Consider the system* (28) *and suppose that f is Lipschitz continuous on the region of attraction $\mathcal{R}_A$ of an asymptotically stable equilibrium point x^*. Then, an open set $\mathcal{G}$ containing x^* coincides with $\mathcal{R}_A$, if and only if there exist two continuous positive definite functions $W : \mathcal{G} \mapsto \mathbb{R}$ and $h : \mathcal{M} \mapsto \mathbb{R}$ such that*

i) $W(x^*) = 0$, $W(x) > 0$ for all $x \in \mathcal{G} \backslash \{x^*\}$,

ii) $W(x) \to 1$ as $x \to \partial\mathcal{G}$ or, in the case of unbounded $\mathcal{G}$, as $d(x, x^*) \to \infty$, where $\partial\mathcal{G}$ is the boundary of $\mathcal{G}$ and $d(.,.)$ is a metric defined on $\mathcal{M}$,

iii) $\dot{W}(x)$ is well defined for all $x \in \mathcal{G}$ and

$$\dot{W}(x) = -h(x)\,(1 - W(x))\,. \tag{32}$$

PROOF. [Theorem 10.] We start by showing that the derivative of V is nonpositive. Substituting (30) in (20) and (21) yields

$$\dot{V} = -k_v n \mathbf{e}^T \mathbf{e} - k_\omega \mathbf{b}_\omega^T \mathbf{b}_\omega.$$

Then, we have $\dot{V} \leq 0$ for all $(\mathbf{e}, R_e) \in \mathrm{SE}(3)$ and $\dot{V} = 0$ for $\mathbf{e} = 0$ and R_e in the set $\mathcal{C}_{V_2}$ already determined in Lemma 7. By Lyapunov's stability theory, we can conclude local stability of $(0, I_3)$ and, by LaSalle's invariance principle, global convergence to the set $\{(\mathbf{e}, R_e) : \mathbf{e} = 0 \text{ and } R_e \in \mathcal{C}_{V_2}\}$. To prove almost global asymptotic stability of $(0, I_3)$, consider the autonomous orientation subsystem resulting from the feedback interconnection of (7b) and (30b), and the continuously differentiable positive definite function

$$\bar{V}_2(R_e) = \mathrm{tr}(I_3 - R_e), \tag{33}$$

which corresponds to (18) with $M = I_3$. Using the angle-axis representation, $R_e = \mathrm{rot}(\theta, \mathbf{n})$, and with an obvious

abuse of notation, $\bar{V}_2$ can be expressed as $\bar{V}_2(\theta) = 2(1 - \cos\theta)$. Using (22) with $P = 2I_3$ and (30b) with the original P, the time derivative $\dot{\bar{V}}_2$ can be written as

$$\dot{\bar{V}}_2 = -2\sin\theta\,\mathbf{n}^T R^* \boldsymbol{\omega} = -2k_\omega(\sin\theta)^2\,\mathbf{n}^T P\mathbf{n} \leq 0. \quad (34)$$

Defining the set $\mathcal{G} = \mathrm{SO}(3)\backslash\mathcal{N}_A$, where $\mathcal{N}_A = \{R_e : \mathrm{tr}(I_3 - R_e) = 4\}$, it is straightforward to show that $W(R_e) = \frac{1}{4}\bar{V}_2(R_e)$ together with $h(R_e) = k_\omega V_2(R_e)$ satisfy the conditions of Theorem 12, therefore implying that $\mathcal{G}$ is the region of attraction for the orientation subsystem and $\mathcal{R}_A$ defined in (31) is the region of attraction for the overall position and orientation closed-loop system. By noting that the set outside the region of attraction can be rewritten as $\mathrm{SE}(3) \setminus \mathcal{R}_A = \{(\mathbf{e}, R_e) : d(I_3, R_e) = 4\}$, where $d(.\,,.)$ is the metric on SO(3) given by

$$\begin{aligned} d : \mathrm{SO}(3) \times \mathrm{SO}(3) &\to [0, 4] \\ (R_1, R_2) &\mapsto \mathrm{tr}(I_3 - R_1^T R_2), \end{aligned} \quad (35)$$

one concludes that $\mathrm{SE}(3) \setminus \mathcal{R}_A$ is a nowhere dense set of measure zero, and therefore $(0, I_3)$ is almost GAS. □

Remark 13 *We can define a bijection between* SO(3) *and a ball in* $\mathbb{R}^3$ *of radius* π*, by assuming that antipodal points on the ball's surface (the sphere of radius* π*) represent the same rotation. For each rotation matrix* $R_e \in \mathrm{SO}(3)$*, there is a unique point* $\theta\mathbf{n}$ *in the interior of the ball,* $0 \leq \theta < \pi$*, or two antipodal points* $\theta\mathbf{n}$ *and* $-\theta\mathbf{n}$ *in the surface,* $\theta = \pi$*, such that* $\mathrm{rot}(\theta, \mathbf{n}) = R_e$*.*

As illustrated in Figure 3, the level surfaces for $\bar{V}_2(R_e) = \mathrm{tr}(I_3 - R_e)$*, or equivalently for* $\bar{V}_2(\theta) = 2(1 - \cos\theta)$*, take the form of spheres of radius* $\theta \in [0, \pi]$*, with a minimum at* $\bar{V}_2(0) = 0$ *and a maximum at* $\bar{V}_2(\pi) = 4$*. Hence, the nowhere dense zero measure set* $\{R_e : \mathrm{tr}(I_3 - R_e) = 4\}$*, which is outside the region of attraction for the rotation system, can be identified with the ball's surface.* □

Remark 14 *When* M *satisfies certain conditions, the function* $V_2(R_e)$ *defined in* (18) *corresponds to the modified trace function on* SO(3) *studied in [11] and [4]. In those works, to prove almost GAS of the desired equilibrium points, the authors rely on the fact that* V_2 *is a Morse function on* SO(3)*, i.e. a function whose critical points are all nondegenerate and consequently isolated [11]. This corresponds to constraining* P*, or equivalently* M*, to have all distinct eigenvalues. In our work, this restriction has been lifted, since the proof of almost GAS follows a different approach. We can therefore consider landmark configurations, which do not yield a Morse function for* V_2 *because their critical points are not isolated. It can be shown that* C_{V_2} *is exactly the set of critical points of* V_2*, i.e. the set of rotations* $R_e \in \mathrm{SO}(3)$ *such that the derivative* $(dV_2)_{R_e} : T_{R_e}\mathrm{SO}(3) \mapsto \mathbb{R}$ *is not surjective. Hence, the function* V_2 *for the square configuration shown in Fig. 2(b) is not a Morse function, since the set* $C_{V_2}^{(2)}$ *given in* (27) *comprises a connected set.* □

Fig. 3. Region of attraction for the rotation system.

3.1. *Properties of the control law*

The first property that we would like to highlight is the fact that the control law (30) can be expressed solely in terms of the current and desired outputs Q and Q^*, respectively.

Lemma 15 *Under Assumption 2, the control law defined*

in (30) *can be rewritten as*

$$\mathbf{v} = k_v(Q - Q^*)\mathbf{a} + S(Q\mathbf{a})\boldsymbol{\omega}, \tag{36a}$$

$$\boldsymbol{\omega} = k_\omega S^{-1}(QD_aQ^{*T} - Q^*D_aQ^T) - k_\omega S(Q^*\mathbf{a})Q\mathbf{a}. \tag{36b}$$

PROOF. Since $Q = RX + \mathbf{p}\mathbf{1}^T$ and, according to Proposition 3, $X\mathbf{a} = 0$ and $\mathbf{1}^T\mathbf{a} = 1$, we have that $Q\mathbf{a} = -\mathbf{p}$ and so (30a) can be rewritten as

$$\mathbf{v} = -k_v\mathbf{e} - S(\mathbf{p})\boldsymbol{\omega} = k_v(Q - Q^*)\mathbf{a} + S(Q\mathbf{a})\boldsymbol{\omega}.$$

To obtain an alternative expression for (30b), note that

$$\begin{aligned}\boldsymbol{\omega} = k_\omega \mathbf{b}_\omega &= k_\omega R^{*T} S^{-1}\left(R_e M - M R_e^T\right) \\ &= k_\omega S^{-1}\left(R^T M R^* - R^{*T} M R\right) \\ &= k_\omega S^{-1}\left(R^T X D_a X^T R^* - R^{*T} X D_a X^T R\right),\end{aligned}$$

and $R^TX = Q(I_n - \mathbf{a}\mathbf{1}^T)$. Then, we can take the expression $R^TXD_aX^TR^*$, rewrite it as

$$\begin{aligned}R^T X D_a X^T R^* &= Q(I_n - \mathbf{a}\mathbf{1}^T)D_a(I_n - \mathbf{1}\mathbf{a}^T)Q^{*T} \\ &= QD_aQ^{*T} - Q\mathbf{a}\mathbf{a}^TQ^{*T},\end{aligned}$$

and use Proposition 21 to obtain

$$\begin{aligned}\boldsymbol{\omega} &= k_\omega S^{-1}(QD_aQ^{*T} - Q^*D_aQ^T) \\ &\quad - k_\omega S^{-1}(Q\mathbf{a}\mathbf{a}^TQ^{*T} - Q^*\mathbf{a}\mathbf{a}^TQ^T) \\ &= k_\omega S^{-1}(QD_aQ^{*T} - Q^*D_aQ^T) - k_\omega S(Q^*\mathbf{a})Q\mathbf{a}.\end{aligned}$$

□

The remaining properties relate to the dynamic behavior of the closed-loop system, which can be rewritten as

$$\dot{\mathbf{e}} = -k_v\mathbf{e} \tag{37a}$$

$$\dot{R}_e = -k_\omega(R_eM - MR_e^T)R_e \tag{37b}$$

We can immediately conclude that the proposed control law decouples the position and orientation errors subsystems and that the position error subsystem (37a) has a globally exponentially stable equilibrium point at $\mathbf{e} = 0$.

Using the metric on SO(3) given by (35), we show next that $R_e = I_3$ is almost globally exponentially stable (GES), in the sense that, for almost all initial conditions, the distance $d(I_3, R_e) = \mathrm{tr}(I_3 - R_e)$ converges exponentially fast to zero.

Lemma 16 *The orientation subsystem* (37b) *has an almost GES equilibrium point at* $R_e = I_3$.

PROOF. Noting that $d(I_3, R_e) = \bar{V}_2(R_e)$ as defined in (33), we can use the expression for $\dot{\bar{V}}_2$ given in (34) to obtain

$$\begin{aligned}\dot{\bar{V}}_2 &= -2k_\omega(\sin\theta)^2\,\mathbf{n}^TP\mathbf{n} \\ &\leq -2k_\omega(1+\cos\theta)(1-\cos\theta)\lambda_1 \\ &= -k_\omega\lambda_1(2 - \frac{1}{2}\bar{V}_2)\bar{V}_2 \leq 0,\end{aligned}$$

where $\lambda_1 > 0$ is the smallest eigenvalue of P. Since $\dot{\bar{V}}_2 \leq 0$, we have $2 - \frac{1}{2}\bar{V}_2(R_e(t)) \geq 2 - \frac{1}{2}\bar{V}_2(R_e(0))$ for all $t \geq 0$. Then, we can write

$$\dot{\bar{V}}_2(R_e(t)) \leq -\alpha\bar{V}_2(R_e(t)),$$

where $\alpha = k_\omega(2 - \frac{1}{2}\bar{V}_2(R_e(0)))\lambda_1$ and $\alpha > 0$ for all $R_e(0)$ such that $V_2(R_e(0)) < 4$, i.e. for all initial conditions inside the region of attraction. □

To further analyze the stability and convergence properties of the orientation subsystem, it is convenient to consider the angle of rotation θ and axis of rotation $\mathbf{n}$ (recall that R_e can be written as $R_e = \mathrm{rot}(\theta, \mathbf{n})$). Note that the convergence of θ to zero is enough to guarantee that R_e converges to I_3. Consequently, analyzing the stability of θ can provide an alternative way of proving Lemma 16. More importantly, analyzing the convergence of $\mathbf{n}$ gives further insight on how the system evolves to the target configuration.

According to Lemma 19 and (7b), for $0 < \theta < \pi$, the time derivatives $\dot{\theta}$ and $\dot{\mathbf{n}}$ are given by

$$\dot{\theta} = -\mathbf{n}^TR^{*T}\boldsymbol{\omega}, \tag{38}$$

$$\dot{\mathbf{n}} = \frac{1}{2}\left(\frac{\sin\theta}{1-\cos\theta}S(\mathbf{n}) + I_3\right)S(\mathbf{n})R^{*T}\boldsymbol{\omega}, \tag{39}$$

respectively. Applying the control law $\boldsymbol{\omega} = k_\omega R^* N(\theta, \mathbf{n}) P\mathbf{n}$, it is straightforward to show that, in closed-loop, (38) and (39) become

$$\dot{\theta} = -k_\omega \sin\theta \ \mathbf{n}^T P\mathbf{n} \tag{40}$$

$$\dot{\mathbf{n}} = k_\omega S(\mathbf{n})^2 P\mathbf{n}, \tag{41}$$

respectively. As stated in Proposition 4, the matrix P defined in (11) is positive definite provided that the landmarks satisfy Assumptions 1 and 2. We can immediately conclude from (40) that the proposed controller guarantees not only the asymptotic convergence of θ to the origin, but also its decreasing monotonicity. Considering now (41), if the landmarks are placed such that all eigenvalues of P are equal, i.e. $P = \alpha I_3$ for some $\alpha > 0$, then $\dot{\mathbf{n}} = 0$ and so the convergence of R to R^* is achieved by rotating along a constant axis of rotation, which is determined by the initial condition of the system. On the other extreme case where all the eigenvalues of P are distinct, we can divide $\mathbb{S}^2$ into the positive and negative half-spaces associated with the smallest eigenvalue of P and show that $\mathbf{n}$ converges to the corresponding eigenvector, with positive or negative sign depending on which of the half-spaces the system is started. The boundary between the two sets constitutes an invariant set of the system. The following result formalizes these considerations and also the intermediate cases where $\lambda_1 = \lambda_2 < \lambda_3$ and $\lambda_1 < \lambda_2 = \lambda_3$.

Lemma 17 *Let $P \in \mathbb{R}^{3\times 3}$ be a positive definite matrix with eigenvalues $0 < \lambda_1 \leq \lambda_2 \leq \lambda_3$. Considering the system (41), three cases may occur:*

i) when $\lambda_1 = \lambda_2 = \lambda_3$, (41) becomes $\dot{\mathbf{n}} = 0$;

ii) when $\lambda_1 < \lambda_2 \leq \lambda_3$, the asymptotically stable equilibrium points of (41) are given by the unitary eigenvectors $\mathbf{n}_1$ and $-\mathbf{n}_1$ associated with λ_1 and $\mathbf{n}(t) \to \text{sign}(\mathbf{n}(0)^T\mathbf{n}_1)\mathbf{n}_1$ as $t \to \infty$, provided that $\mathbf{n}(0)^T\mathbf{n}_1 \neq 0$;

iii) when $\lambda_1 = \lambda_2 < \lambda_3$, the asymptotically stable equilibrium points form the set $\{\mathbf{n} : \mathbf{n} \in \text{span}(\mathbf{n_1}, \mathbf{n}_2) \cap \mathbb{S}^2\}$ and the system converges to a point in this set provided that $\mathbf{n}(0) \neq \pm\mathbf{n}_3$.

PROOF. To analyze the stability of (41) when $\lambda_1 < \lambda_2 \leq \lambda_3$, consider the candidate Lyapunov function $V(\mathbf{n}(t)) = 1 - \mathbf{n}_1^T\mathbf{n}(t)$, with unique maximum at $V(-\mathbf{n}_1) = 2$ and unique minimum at $V(\mathbf{n}_1) = 0$. According to (41), $\dot{V}$ is given by

$$\begin{aligned}\dot{V} &= -k_\omega \mathbf{n}_1^T S(\mathbf{n})^2 P\mathbf{n} \\ &= -k_\omega \mathbf{n}_1^T \mathbf{n}(\mathbf{n}^T P\mathbf{n} - \lambda_1) \\ &= -k_\omega (\mathbf{n}^T P\mathbf{n} - \lambda_1)(1 - V).\end{aligned}$$

Then, if $\mathbf{n}^T P\mathbf{n} > \lambda_1$ and $V < 1$, we have $\dot{V} < 0$. These conditions are equivalent to $\mathbf{n} \neq \pm\mathbf{n}_1$ and $\mathbf{n}_1^T\mathbf{n} > 0$, respectively. It follows that the system verifies the conditions of Zubov's Theorem with $\mathcal{G} = \{\mathbf{n} \in \mathbb{S}^2 : \mathbf{n}_1^T\mathbf{n} > 0\}$, $W(\mathbf{n}) = V(\mathbf{n})$, and $h(\mathbf{n}) = k_\omega(\mathbf{n}^T P\mathbf{n} - \lambda_1)$, and therefore $\mathbf{n}_1$ is asymptotically stable with region of attraction given by $\mathcal{G}$. The same argument but with $V(\mathbf{n}(t)) = 1 + \mathbf{n}_1^T\mathbf{n}(t)$ can be used to prove that $-\mathbf{n}_1$ is asymptotically stable, with region of attraction given by $\bar{\mathcal{G}} = \{\mathbf{n} \in \mathbb{S}^2 : \mathbf{n}_1^T\mathbf{n} < 0\}$.

Considering now the case when $\lambda_1 = \lambda_2 < \lambda_3$, it is straightforward to show that $V(\mathbf{n}(t)) = 1 - \mathbf{n}(t)^T(\mathbf{n}_1\mathbf{n}_1^T + \mathbf{n}_2\mathbf{n}_2^T)\mathbf{n}(t)$ is a Lyapunov function for the system, with derivative given by $\dot{V} = -k_\omega(\mathbf{n}^T P\mathbf{n} - \lambda_1)(1 - V)$ and maximum at $V(\pm\mathbf{n}_3) = 1$. Applying Zubov's Theorem, we can conclude that the set of asymptotically stable equilibria is given by $\{\mathbf{n} \in \mathbb{S}^2 : V(\mathbf{n}) = 0\} = \{\mathbf{n} \in \mathbb{S}^2 : \mathbf{n} \in \text{span}(\mathbf{n}_1, \mathbf{n}_2)\}$ and that $\mathcal{G} = \{\mathbf{n} \in \mathbb{S}^2 : \mathbf{n} \neq \pm\mathbf{n}_3\}$ defines the region of attraction. □

This lemma turns out to be a very useful result, because it tells us how to select the axis of rotation to which $\mathbf{n}$ converges, by choosing a particular placement for the landmarks. This will be further illustrated in Section 4 through examples.

3.2. *Tracking control around fixed landmarks*

The approach proposed for stabilization on SE(3) can be extended to solve a trajectory-tracking problem, in which the rigid body is required to follow a moving configuration using measurements originating from fixed landmarks. In this setting, the desired configuration $(\mathbf{p}^*, R^*) \in \mathrm{SE}(3)$ is no longer fixed in the environment. Instead, it is assumed that, given an initial condition $(\mathbf{p}^*(0), R^*(0)) \in \mathrm{SE}(3)$, $(\mathbf{p}^*, R^*)$ evolves according to an exosystem of the following form

$$\dot{\mathbf{p}}^* = \mathbf{v}^* - S(\boldsymbol{\omega}^*)\mathbf{p}^* \tag{42a}$$

$$\dot{R}^* = R^* S(\boldsymbol{\omega}^*), \tag{42b}$$

where the reference velocities $\mathbf{v}^*$ and $\boldsymbol{\omega}^*$ are assumed to be continuously differentiable and bounded functions of time. The motion of the elements $\mathbf{q}_j^*$ of the desired output matrix $Q^* = [\mathbf{q}_1 \ \dots \ \mathbf{q}_n]$ is then governed by $\dot{\mathbf{q}}_j^* = -\mathbf{v}^* - S(\boldsymbol{\omega}^*)\mathbf{q}_j^*$ and the error model defined in (7) becomes

$$\dot{\mathbf{e}} = \mathbf{v} - \mathbf{v}^* - S(\boldsymbol{\omega})(\mathbf{e} + \mathbf{p}^*) + S(\boldsymbol{\omega}^*)\mathbf{p}^* \tag{43a}$$

$$\dot{R}_e = -S(R^*(\boldsymbol{\omega} - \boldsymbol{\omega}^*))R_e. \tag{43b}$$

Considering once more the candidate Lyapunov function $V = V_1(\mathbf{e}) + V_2(R_e)$ defined in (16-18) and performing very similar computations to those of Lemma 6, it is straightforward to show that the time derivatives of V_1 and V_2 are now given by

$$\dot{V}_1 = n\mathbf{e}^T(\mathbf{v} - \mathbf{v}^* + S(\mathbf{p}^*)(\boldsymbol{\omega} - \boldsymbol{\omega}^*)) \tag{44}$$

and

$$\dot{V}_2 = -S^{-T}(R_e M - M R_e^T)R^*(\boldsymbol{\omega} - \boldsymbol{\omega}^*), \tag{45}$$

respectively. These immediately suggest the definition of a feedback law by similarity with (30), which is given by

$$\mathbf{v} = \mathbf{v}^* - k_v\mathbf{e} - S(\mathbf{e} + \mathbf{p}^*)\boldsymbol{\omega} + S(\mathbf{p}^*)\boldsymbol{\omega}^*, \tag{46a}$$

$$\boldsymbol{\omega} = \boldsymbol{\omega}^* + k_\omega R^{*T} S^{-1}(R_e M - M R_e^T), \tag{46b}$$

and can be expressed in terms of the output as

$$\mathbf{v} = \mathbf{v}^* + k_v(Q - Q^*)\mathbf{a} + S(Q\mathbf{a})\boldsymbol{\omega} - S(Q^*\mathbf{a})\boldsymbol{\omega}^*, \tag{47a}$$

$$\boldsymbol{\omega} = \boldsymbol{\omega}^* + k_\omega S^{-1}(Q D_a Q^{*T} - Q^* D_a Q^T) - k_\omega S(Q^*\mathbf{a})Q\mathbf{a}. \tag{47b}$$

As stated in the following corollary of Theorem 10, the control law defined in (47) ensures almost global asymptotic tracking of the reference $(\mathbf{p}^*, R^*)$.

Corollary 18 *The closed-loop system resulting from the interconnection of* (43) *and* (46) *has an almost GES equilibrium point at* $(\mathbf{e}, R_e) = (0, I_3)$*, for any positive* k_v *and* k_ω*. The corresponding region of attraction is given by* $\mathcal{R}_A = \mathrm{SE}(3) \setminus \{(\mathbf{e}, R_e) : \mathrm{tr}(I_3 - R_e) = 4\}$.

PROOF. Note that the interconnection of (43) and (46) results in an autonomous system of the form

$$\dot{\mathbf{e}} = -k_v\mathbf{e}$$

$$\dot{R}_e = -k_\omega(R_e M - M R_e^T)R_e.$$

Since the closed-loop system is exactly the same as the one considered in Theorem 10 and Lemma 16, we can conclude that it has an almost GES equilibrium point at $(\mathbf{e}, R_e) = (0, I_3)$, with region of attraction given by (31). □

4. Simulation results

In this section, we present simulation results that corroborate the stability characteristics of the system and illustrate the properties discussed in the preceding sections. We consider two different landmark configurations, corresponding to matrices

$$X_1 = \begin{bmatrix} 1 & 1 & -1 & -1 \\ 2 & -2 & -2 & 2 \\ 0 & 0 & 0 & 0 \end{bmatrix}, \ X_2 = \begin{bmatrix} 0 & 0 & 0 & 0 \\ 1 & -1 & -1 & 1 \\ 2 & 2 & -2 & -2 \end{bmatrix}.$$

Note that in both cases, the origin of $\{I\}$ coincides with the landmark's centroid and therefore satisfies Assumption 2. It also follows that $X_1\mathbf{1} = X_2\mathbf{1} = 0$ and therefore $\mathbf{a} = \frac{1}{n}\mathbf{1}$ and $D_a = \frac{1}{n}I_n$ for both matrices. Figures 4(a) and (b) show

the trajectories described by the system using control laws based on X_1 and X_2, respectively. Both were initialized at the same position and orientation and share the same target state $(\mathbf{p}^*, R^*) = ([0\ 0\ -10]^T, I_3)$.

(a) Trajectory resulting from the landmarks in X_1.

(b) Trajectory resulting from the landmarks in X_2.

Fig. 4. System trajectories for the examples in Section 4.

We can see that, in both cases, the system starts by describing an almost straight-line trajectory in position, which reflects the quick convergence of the position error $\mathbf{e}$ to a small neighborhood of the origin. From then on, the behavior of the system is very much determined by the attitude controller, since the position evolves so as to maintain $\mathbf{e}$ close to zero. At this point, the difference between trajectories becomes more pronounced. This behavior is directly related to the placement of the landmarks. As shown in Figure 5, when X_1 is used, the axis of rotation converges to $[0\ -1\ 0]^T$ (solid line) whereas when X_2 is used, it converges to $[0\ 0\ 1]^T$ (dotted line). We recall that each of these vectors corresponds to the eigenvector associated with the smallest eigenvalue of $P_1 = \frac{1}{n}\text{tr}(X_1X_1^T)I_3 - \frac{1}{n}X_1X_1^T$ and $P_2 = \frac{1}{n}\text{tr}(X_2X_2^T)I_3 - \frac{1}{n}X_2X_2^T$, respectively.

Fig. 5. Time evolution for angle-axis pair $(\theta, \mathbf{n})$.

The result obtained suggests that a careful placement of the landmarks with respect to the desired configuration can give rise to "better-behaved" trajectories. More specifically, if X is selected such that the axis of rotation converges to

$\pm\mathbf{p}^*/\|\mathbf{p}^*\|$ (in the example, X_2 verifies this condition), the last stage of convergence will only involve a rotation about that axis, producing no translational motion.

To illustrate the type of results that can be obtained with the tracking controller and assess the robustness with respect to measurement noise, we consider the case where the system is supposed to track a circular trajectory based on noisy measurements of the landmark configuration X_2. Figure 6(a) shows the trajectory described by the system when the initial position and orientation in the inertial frame are set to ${}^I\mathbf{p}_B = [45\ 45\ -38]^T$ and ${}^I_BR = \mathrm{rot}(2.8, [0.50\ 0.41\ -0.76]^T)$, respectively, which corresponds to an initial error state given by $\mathbf{e} = [-19.2\ -18.5\ 40.9]^T$ and $R_e = \mathrm{rot}(3.1, [-0.52\ -0.09\ 0.85]^T)$. The measurements were corrupted with additive Gaussian noise with a standard deviation of 0.3 m.

It is interesting to note that the system converges fairly quickly to a small neighborhood of the circumference but lags behind the reference roughly until $t = 100$s (see Figure 6(b)). This result can be explained by analyzing the convergence of the error variables $\mathbf{e}$, θ, and $\theta\mathbf{n}$ shown in Figure 7. We can observe that $\mathbf{e}$ has a faster convergence than θ and thus the former determines the initial convergence to the curve, whereas the latter determines the convergence to the actual reference.

Once again, the landmarks' placement has a significant effect on shaping the system's behavior, since the convergence of $\mathbf{n}$ to $[0\ 0\ 1]^T$ ensures that as long as $\mathbf{e}$ is at the origin, the system will be on the circumference irrespective of the value taken by θ.

(a) 3-D view of system trajectory.

(b) Positions in $\{I\}$: ${}^I\mathbf{p}_B$ (thick lines) and ${}^I\mathbf{p}_D$ (thin lines).

Fig. 6. Tracking a circular trajectory based on X_2.

5. Conclusions

In this paper, a Lyapunov-based output-feedback controller for the stabilization of systems evolving on SE(3) was introduced. The solution proposed guarantees almost GES of the desired equilibrium point, i.e. the point is stable and except for a nowhere dense set of zero measure all initial conditions converge exponentially fast to it. The rigid body stabilization problem was defined in a setup of practical significance, by assuming that the output vector matches the type of measurements produced by a number of different on-board sensors. Results were established that describe the dependence of the rotation axis' convergence on the placement of the landmarks. An extension of the

(a) Position error $\mathbf{e} = [e_x\, e_y\, e_z]^T$ and orientation error θ.

(b) Angle-axis error $\theta\mathbf{n}$.

Fig. 7. Time evolution for the position and orientation errors.

output-feedback stabilizing controller was also proposed to address the problem of tracking a moving reference, based on measurements of inertially fixed landmarks.

The work presented in this paper offers new opportunities for further research. Building on the premise that sensor information can be used directly to define relevant error measures and feedback laws, several challenges can be put forward. First, although simulations show that our controller appears to be robust with respect to input disturbances and measurement noise, it remains to prove that this is so and to determine which tradeoffs are involved in making the system robust with respect to this type of disturbances. A second challenge is to go from stabilization to reference-tracking. This problem was briefly touched upon in Section 3.2, but the proposed solution has the limitation of constraining the landmarks to be inertially fixed. An interesting (unsolved) problem would be that of designing an output-feedback controller to maintain the rigid body at a fixed position relative to a collection of moving landmarks. The introduction of a dynamic model is another fundamental topic that requires special attention. Extending the almost global stability result from a kinematic to a dynamic setting may prove to be a challenging problem, specially for the case of underactuated systems with second-order nonholonomic constraints [18]. Finally, the prospect of applying the principles set forth in this paper to tackle the problem of rigid body attitude and position estimation is also very promising.

Acknowledgments

This work was partially supported by Fundação para a Ciência e a Tecnologia (ISR/IST pluriannual funding) through the POS_Conhecimento Program that includes FEDER funds and by the PTDC/EEA-ACR/72853/2006 HELICIM project. Hespanha was partially supported by the National Science Foundation under Grant No. CNS-0720842.

Appendix A. Parameterizing SO(3)

The attitude of a rigid body in the Euclidean Space $\mathbb{E}^3$ can be represented by a rotation matrix describing the relative orientation between a coordinate frame attached to the body and an inertial reference frame. A rotation matrix is an element of the special orthogonal group SO(3), defined as

$$\mathrm{SO}(3) \triangleq \{R \in \mathbb{R}^{3\times 3} : R^T R = I_3 \wedge \det(R) = 1\},$$

i.e., a rotation matrix $R \in \mathrm{SO}(3)$ satisfies the orthogonality condition $R^T R = I_3$ and the orientation-preserving condition $\det(R) = 1$.

It is well-known that SO(3) admits several different parameterizations [16]. In this paper, we adopt the angle-axis representation, which identifies an angle of rotation $\theta \in [0, \pi]$ and an axis of rotation $\mathbf{n} \in \mathbb{S}^2 \triangleq \{\mathbf{x} \in \mathbb{R}^3 : \mathbf{x}^T\mathbf{x} = 1\}$ with an element of SO(3), according to the map defined in (15). Given the kinematic equation of motion for R, we can obtain expressions for $\dot{\theta}$ and $\dot{\mathbf{n}}$ as specified in the following lemma.

Lemma 19 *Let $R \in \mathrm{SO}(3)$ be a rotation of angle θ about the axis $\mathbf{n}$, whose time evolution is described by $\dot{R} = -S(\boldsymbol{\omega})R$. Then, for $0 < \theta < \pi$, the time derivatives of θ and $\mathbf{n}$ can be written as*

$$\dot{\theta} = -\mathbf{n}^T\boldsymbol{\omega}, \tag{A.1}$$

$$\dot{\mathbf{n}} = \frac{1}{2}\left(\frac{\sin\theta}{1-\cos\theta}S(\mathbf{n}) + I_3\right)S(\mathbf{n})\boldsymbol{\omega}, \tag{A.2}$$

respectively.

PROOF. Consider the function $\bar{V}_2 = \mathrm{tr}(I - R) = 2(1 - \cos\theta)$. Taking the time derivative of $\bar{V}_2$ yields

$$-2\sin\theta\mathbf{n}^T\boldsymbol{\omega} = 2\dot{\theta}\sin\theta$$

$$\dot{\theta} = -\mathbf{n}^T\boldsymbol{\omega}, \quad \theta \neq k\pi,\ k \in \mathbb{Z}.$$

To derive an expression for $\dot{\mathbf{n}}$, note that $\mathbf{n}$ is an eigenvector of R associated with a unitary eigenvalue, and therefore $R\mathbf{n} = \mathbf{n}$. Taking the time derivative of this equation yields

$$\dot{R}\mathbf{n} + R\dot{\mathbf{n}} = \dot{\mathbf{n}} \Leftrightarrow -S(\boldsymbol{\omega})R\mathbf{n} = (I_3 - R)\dot{\mathbf{n}}$$

$$\Leftrightarrow S(\mathbf{n})\boldsymbol{\omega} = (-\sin\theta S(\mathbf{n}) - (1-\cos\theta)(\mathbf{n}\mathbf{n}^T - I_3))\dot{\mathbf{n}}$$

Since $\mathbf{n}$ is unitary, we have that $\mathbf{n}^T\dot{\mathbf{n}} = 0$ and so we can write

$$A(\theta,\mathbf{n})\dot{\mathbf{n}} = S(\mathbf{n})\boldsymbol{\omega},\ A(\theta,\mathbf{n}) = -\sin\theta S(\mathbf{n}) + (1-\cos\theta)I_3.$$

Noting that $A(\theta,\mathbf{n})$ is non-singular for $0 < |\theta| < \pi$ and assuming that A^{-1} takes the form $A^{-1} = aS(\mathbf{n}) + b\mathbf{n}\mathbf{n}^T + cI_3$, for some a, b,and $c \in \mathbb{R}$, we can solve $AA^{-1} = I_3$ for these scalars to obtain $a = \frac{1}{2}\frac{\sin\theta}{1-\cos\theta}$, $b = \frac{1}{2}\frac{1+\cos\theta}{1-\cos\theta}$, and $c = \frac{1}{2}$. Then, the derivative of $\mathbf{n}$ can be written as

$$\dot{\mathbf{n}} = A^{-1}(\theta,\mathbf{n})S(\mathbf{n})\boldsymbol{\omega} = \frac{1}{2}\left(\frac{\sin\theta}{1-\cos\theta}S(\mathbf{n}) + I_3\right)S(\mathbf{n})\boldsymbol{\omega}.$$

□

Appendix B. Auxiliary results

Proposition 20 *For all $\mathbf{a} \in \mathbb{R}^3$ and $B \in \mathbb{R}^{3\times 3}$, $\mathrm{tr}(S(\mathbf{a})B) = -\mathbf{a}^T\mathbf{b}$, where $\mathbf{b} = S^{-1}(B - B^T)$.*

PROOF.

$$\begin{aligned}\mathrm{tr}\,(S(\mathbf{a})B) &= \frac{1}{2}\mathrm{tr}\,(S(\mathbf{a})(B - B^T)) + \frac{1}{2}\mathrm{tr}\,(S(\mathbf{a})(B + B^T))\\ &= \frac{1}{2}\mathrm{tr}\,(S(\mathbf{a})S(\mathbf{b})) + \frac{1}{2}\mathrm{tr}\,(S(\mathbf{a})(B - B))\\ &= \frac{1}{2}\mathrm{tr}\,(\mathbf{b}\mathbf{a}^T - \mathbf{a}^T\mathbf{b}I_3) = -\mathbf{a}^T\mathbf{b}\end{aligned}$$

□

Proposition 21 *For all $\mathbf{a}, \mathbf{b} \in \mathbb{R}^3$, $S^{-1}(\mathbf{a}\mathbf{b}^T - \mathbf{b}\mathbf{a}^T) = S(\mathbf{b})\mathbf{a}$.*

PROOF. $\mathbf{c}^T S^{-1}(\mathbf{a}\mathbf{b}^T - \mathbf{b}\mathbf{a}^T) = -\mathrm{tr}(S(\mathbf{c})\mathbf{a}\mathbf{b}^T) = -\mathbf{b}^T S(\mathbf{c})\mathbf{a} = \mathbf{c}^T S(\mathbf{b})\mathbf{a}$ □

References

[1] D. Angeli, Almost global stabilization of the inverted pendulum via continuous state feedback, Automatica 37 (7) (2001) 1103–1108.

[2] D. Angeli, An almost global notion of input-to-state stability, IEEE Transactions on Automatic Control 49 (6) (2004) 866–874.

[3] S. P. Bhata, D. S. Bernstein, A topological obstruction to continuous global stabilization of rotational motion and the unwinding phenomenon, Systems and Control Letters 39 (1) (2000) 63–70.

[4] F. Bullo, A. D. Lewis, Geometric control of mechanical systems, vol. 49 of Texts in Applied Mathematics, Springer, New York, 2004.

[5] N. A. Chaturvedi, A. M. Bloch, N. H. McClamroch, Global stabilization of a fully actuated mechanical system on a riemannian manifold: Controller structure, in: Proceedings of the American Control Conference, Minneapolis, 2006.

[6] N. A. Chaturvedi, N. H. McClamroch, Almost global attitude stabilization of an orbiting satellite including gravity gradient and control saturation effects, in: Proceedings of the American Control Conference, Minneapolis, 2006.

[7] N. J. Cowan, J. D. Weingarten, D. E. Koditschek, Visual servoing via navigation functions, IEEE Transactions on Robotics and Automation 18 (4) (2002) 521–533.

[8] R. Cunha, C. Silvestre, J. Hespanha, Output-feedback control for point stabilization on SE(3), in: IEEE Conference on Decision and Control, San Diego, CA, 2006.

[9] A. Isidori, L. Marconi, A. Serrani, Robust autonomous guidance: an internal model approach, Advances in industrial control, Springer, London, 2003.

[10] H. Khalil, Nonlinear Systems, Third Edition, Prentice Hall, New Jersey, 2000.

[11] D. E. Koditschek, The application of total energy as a lyapunov function for mechanical control systems, in: J. E. Marsden, P. S. Krishnaprasad, J. C. Simo (eds.), Dynamics and Control of Multibody Systems, vol. 97 of Contemporary Mathematics, American Mathematical Society, 1989, pp. 131–158.

[12] M. Lovera, A. Astolfi, Spacecraft attitude control using magnetic actuators, Automatica 40 (8) (2004) 1405–1414.

[13] M. Malisoff, M. Krichman, E. Sontag, Global stabilization for systems evolving on manifolds, Journal of Dynamical and Control Systems 12 (2) (2006) 161–184.

[14] E. Malis, F. Chaumette, Theoretical improvements in the stability analysis of a new class of model-free visual servoing methods, IEEE Transactions on Robotics and Automation 18 (2) (2002) 176–186.

[15] P. Morin, C. Samson, Time-varying exponential stabilization of a rigid spacecraft with two control torques, IEEE Transactions on Automatic Control 42 (4) (1997) 528–534.

[16] R. M. Murray, Z. Li, S. S. Sastry, A Mathematical Introduction to Robotic Manipulation, CRC Press, Florida, 1994.

[17] A. Rantzer, A dual to Lyapunov's stability theorem, Systems and Control Letters 42 (3) (2001) 161–168.

[18] M. Reyhanoglu, A. van der Schaft, N. H. McClamroch, I. Kolmanovsky, Dynamics and control of a class of underactuated mechanical systems, IEEE Transactions on Automatic Control 44 (9) (1999) 1663–1671.

[19] S. Sastry, Nonlinear Systems: Analysis, Stability and Control, Interdisciplinary Applied Mathematics, Springer, New York, 1999.

[20] A. Vannelli, M. Vidyasagar, Maximal lyapunov functions and domains of attraction for autonomous nonlinear systems, Automatica 21 (1) (1985) 69–80.

[21] J. T.-Y. Wen, K. Kreutz-Delgado, The attitude control problem, IEEE Transactions on Automatic Control 36 (10) (1991) 1148–1162.

Figure 1

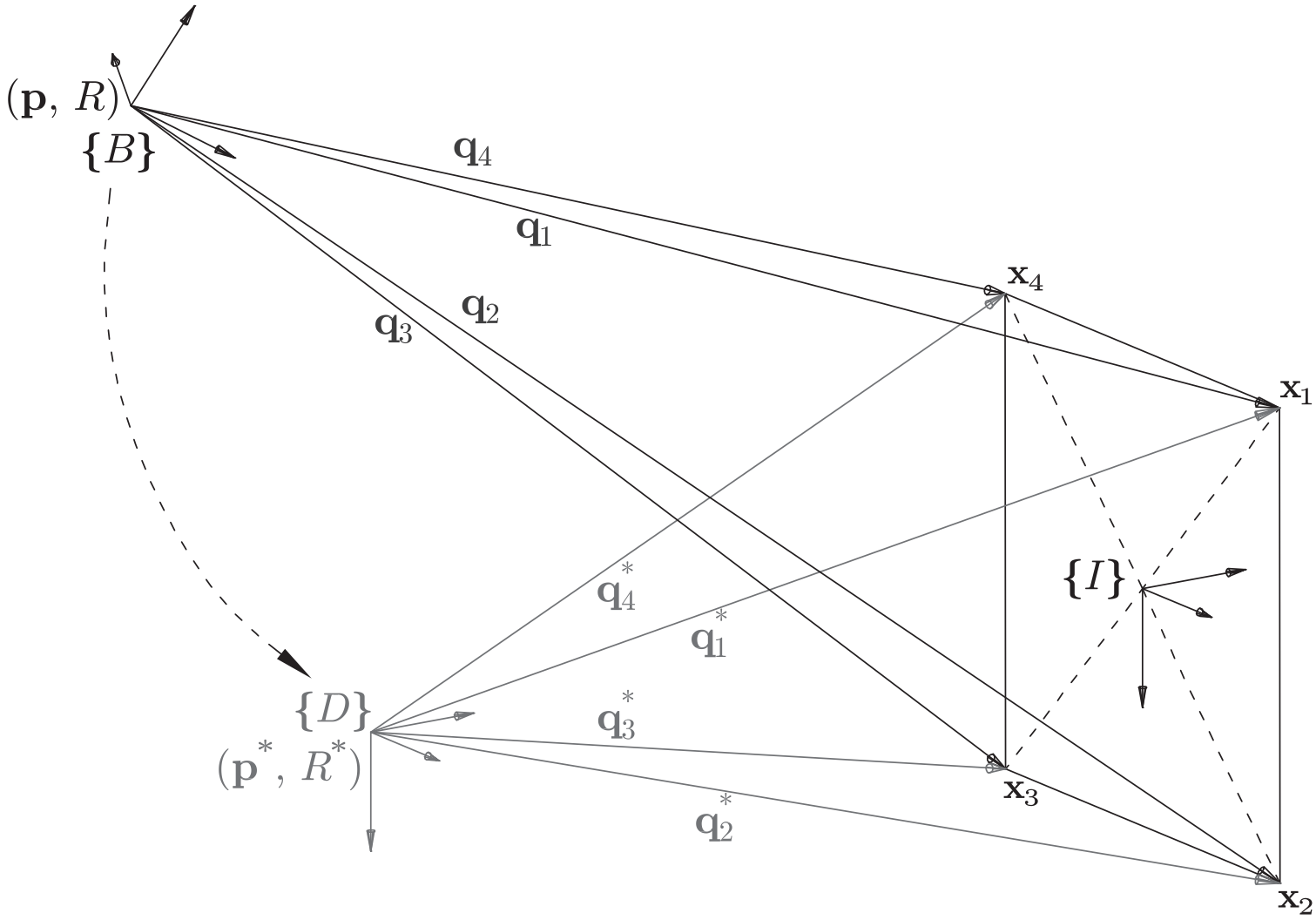

Figure 2a

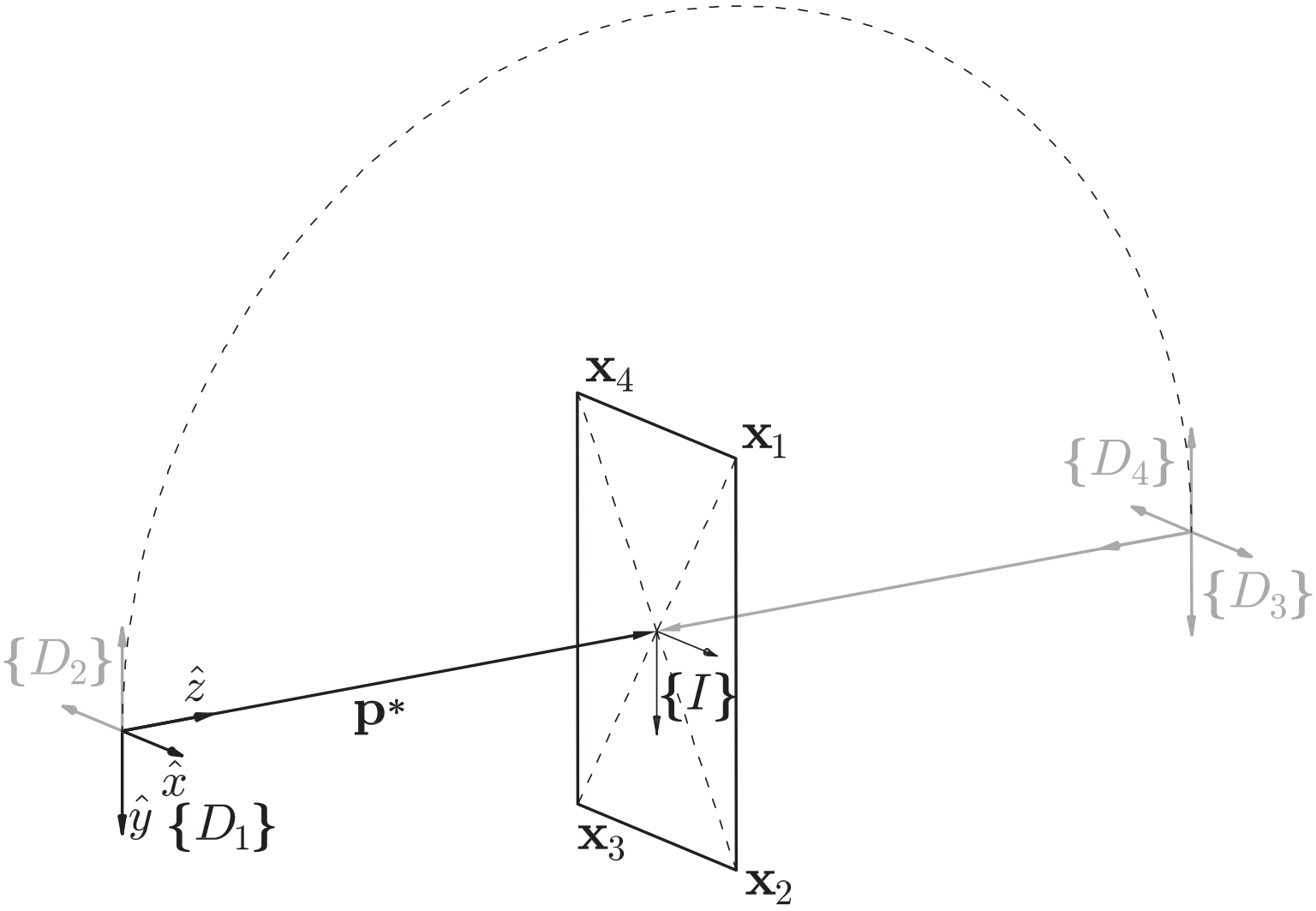
$\mathbf{x}_4$
$\mathbf{x}_1$
$\mathbf{x}_3$
$\mathbf{x}_2$
$\{D_4\}$
$\{D_3\}$
$\{D_2\}$
$\hat{z}$
$\mathbf{p}^*$
$\{I\}$
$\hat{x}$
$\hat{y}$
$\{D_1\}$

Figure 2b

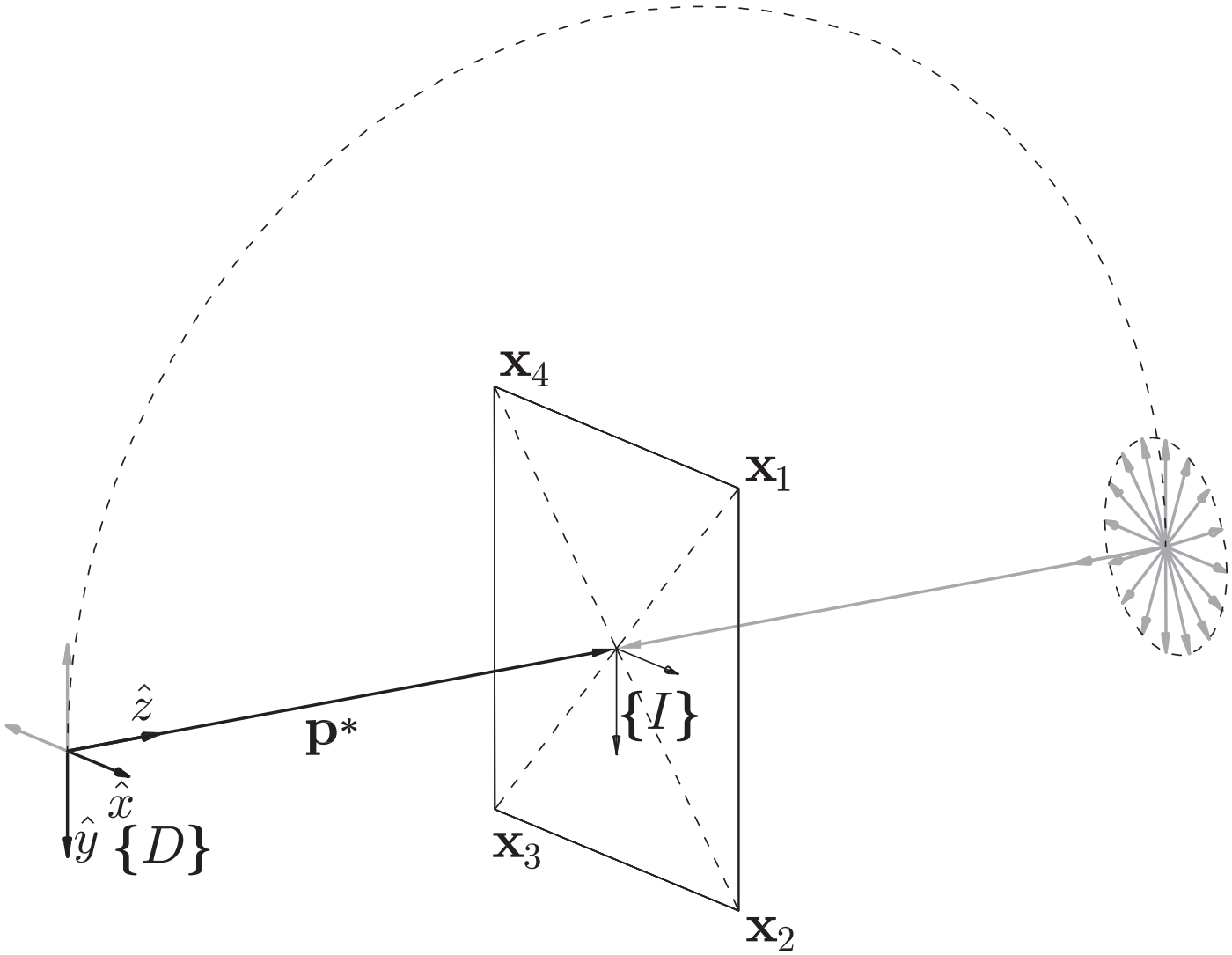
$\mathbf{x}_4$
$\mathbf{x}_1$
$\hat{z}$
$\mathbf{p}^*$
$\{I\}$
$\hat{x}$
$\hat{y}$
$\{D\}$
$\mathbf{x}_3$
$\mathbf{x}_2$

Figure 3

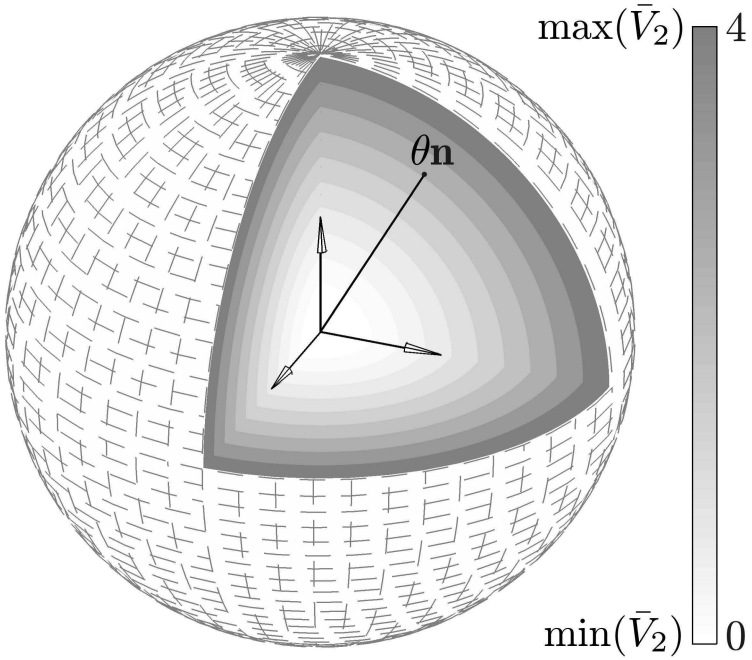

Figure 4a

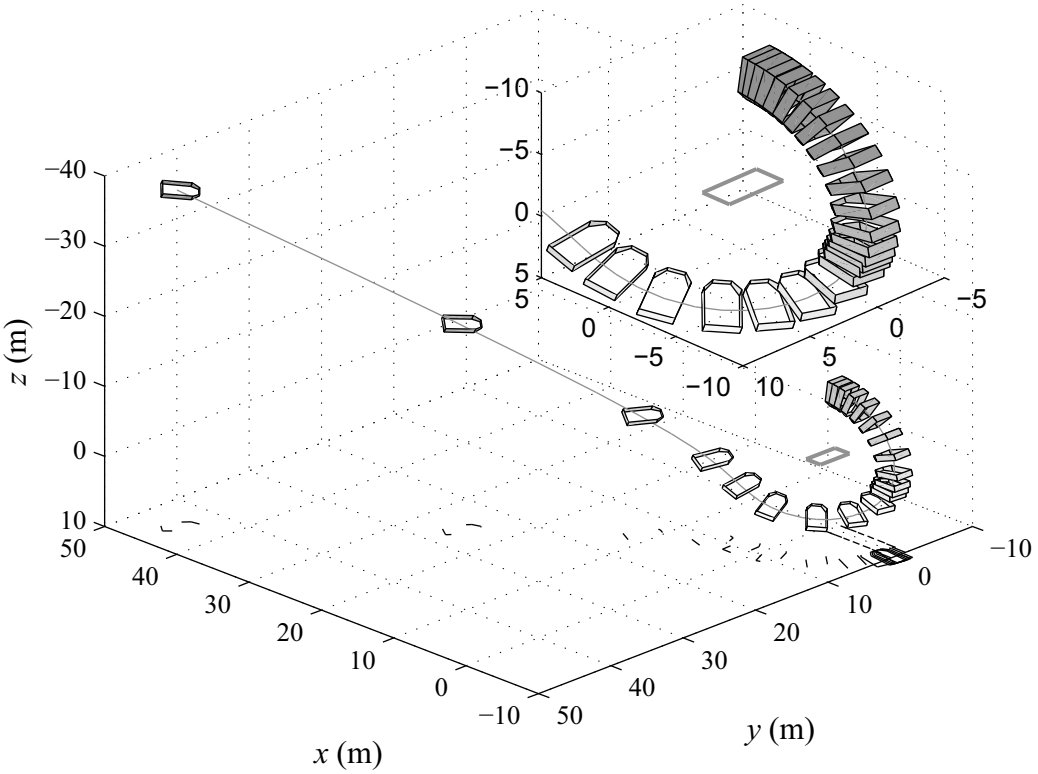
−10
−5
0
5
5
0
−5
−10
10
−5
0
5
−40
−30
−20
−10
0
10
z (m)
50
40
30
20
10
0
−10
x (m)
50
40
30
20
10
0
−10
y (m)

Figure 4b

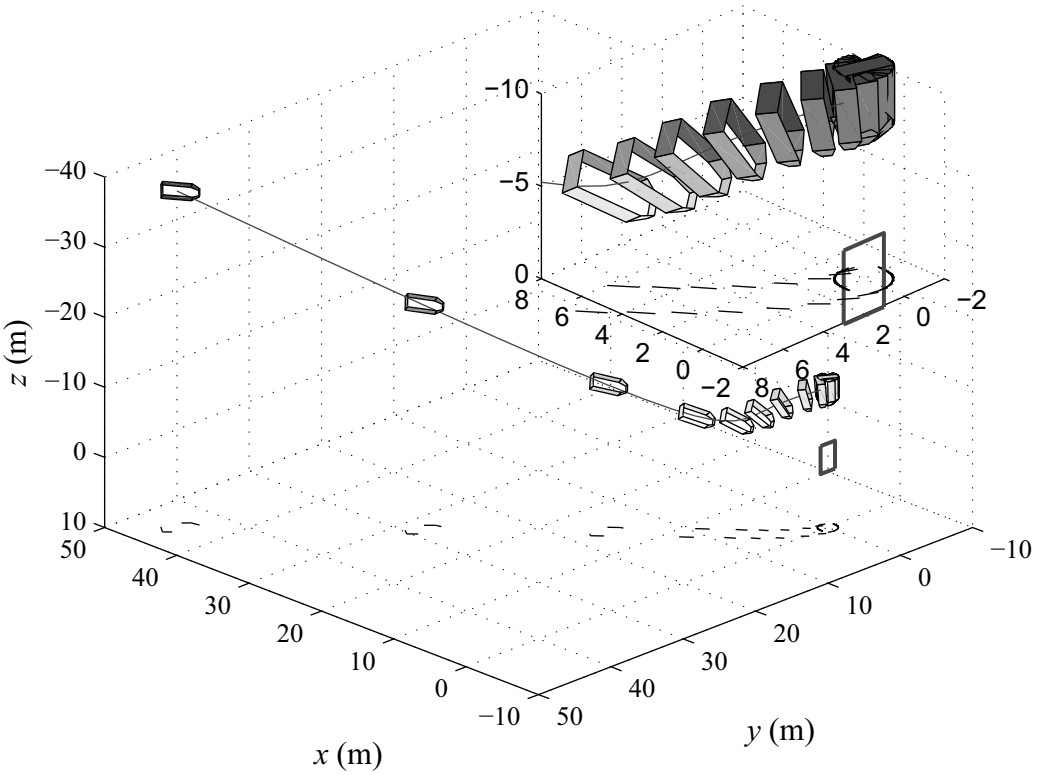
−10
−5
0
8
6
4
2
0
−2
−2
0
2
4
6
8
−40
−30
−20
−10
0
10
z (m)
50
40
30
20
10
0
−10
x (m)
50
40
30
20
10
0
−10
y (m)

Figure 5a

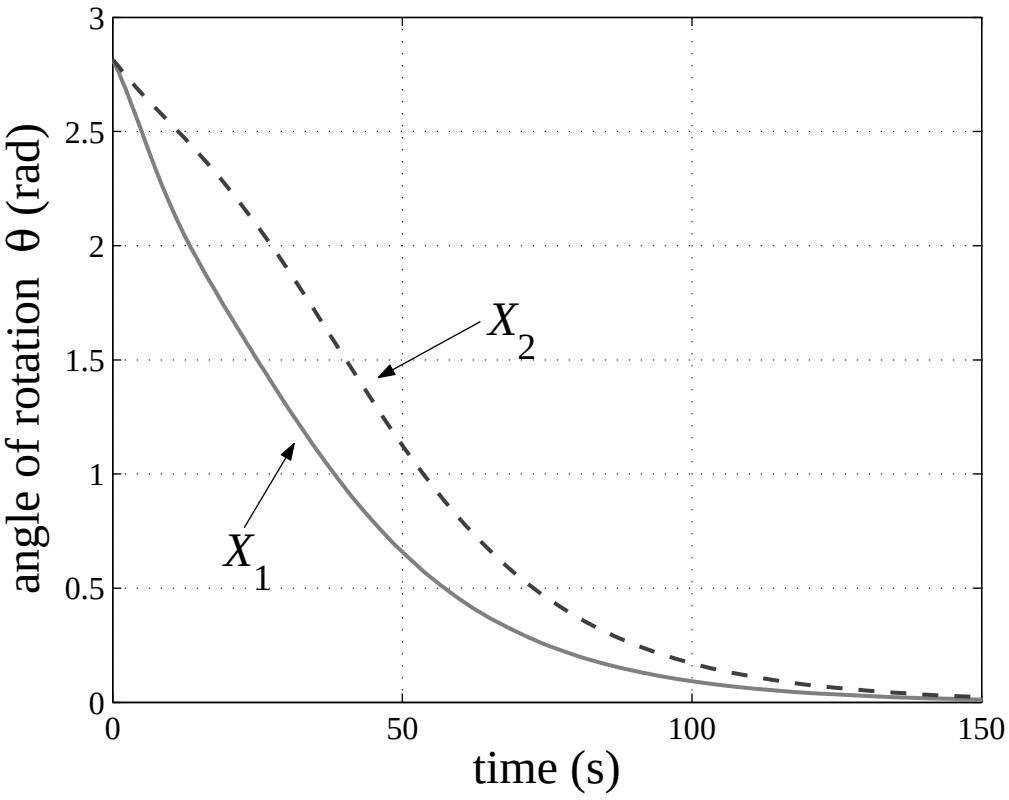

Figure 5b

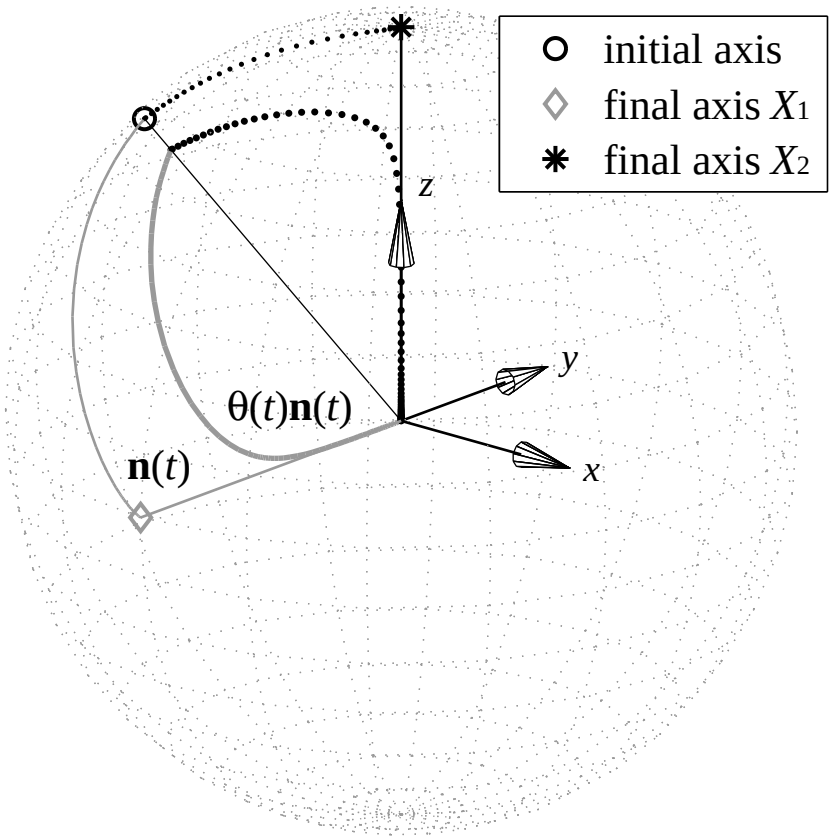

Figure 6a

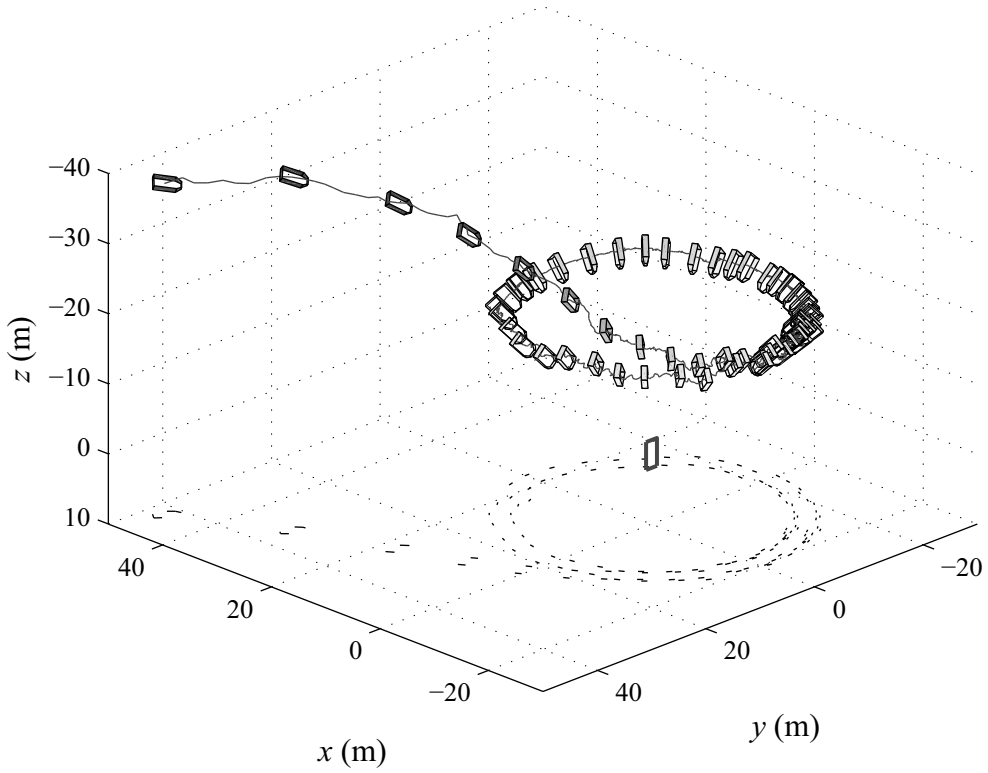

Figure 6b

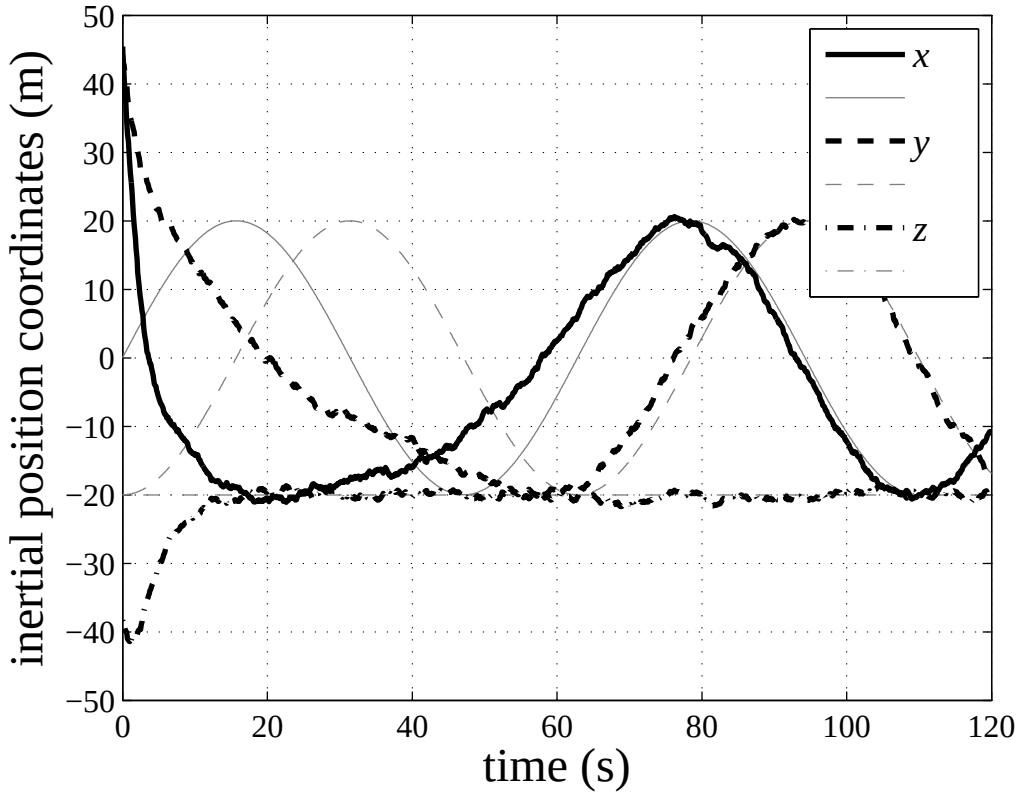
inertial position coordinates (m)
time (s)
x
y
z
50
40
30
20
10
0
−10
−20
−30
−40
−50
0
20
40
60
80
100
120

Figure 7a

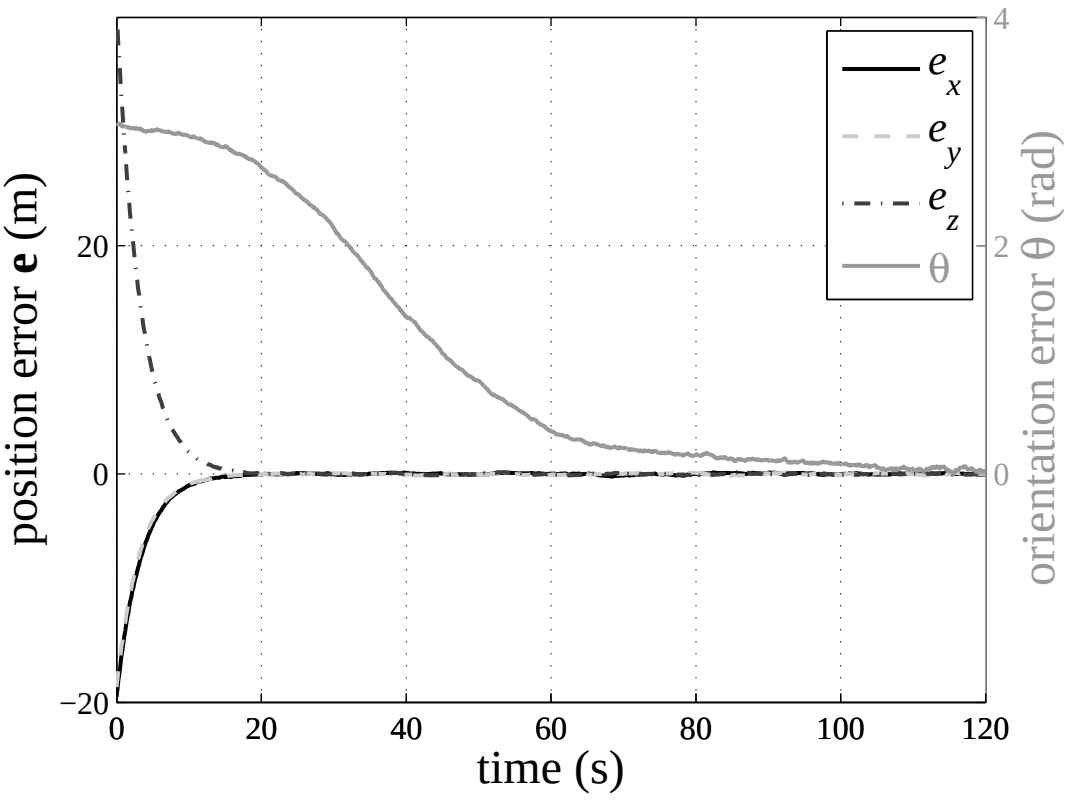
position error **e** (m)
orientation error θ (rad)
time (s)
e_x
e_y
e_z
θ
20
0
−20
2
4
0
20
40
60
80
100
120

Figure 7b

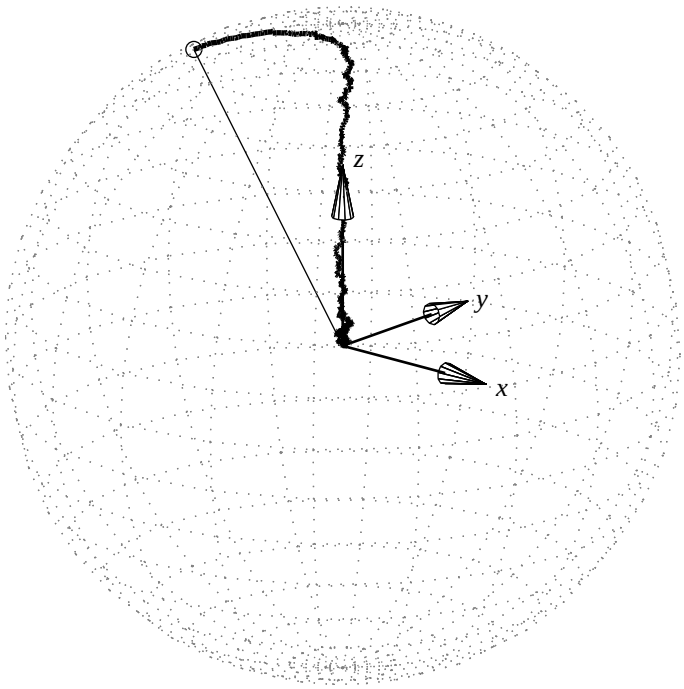

Figure 4a (color)

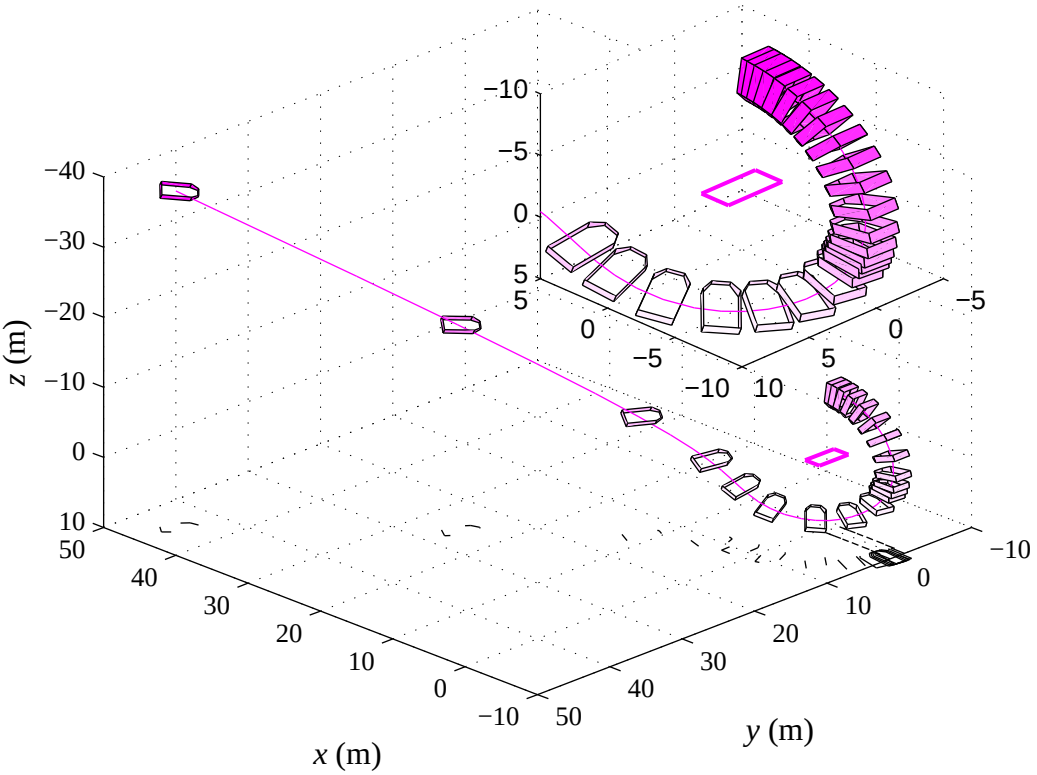

Figure 4b (color)

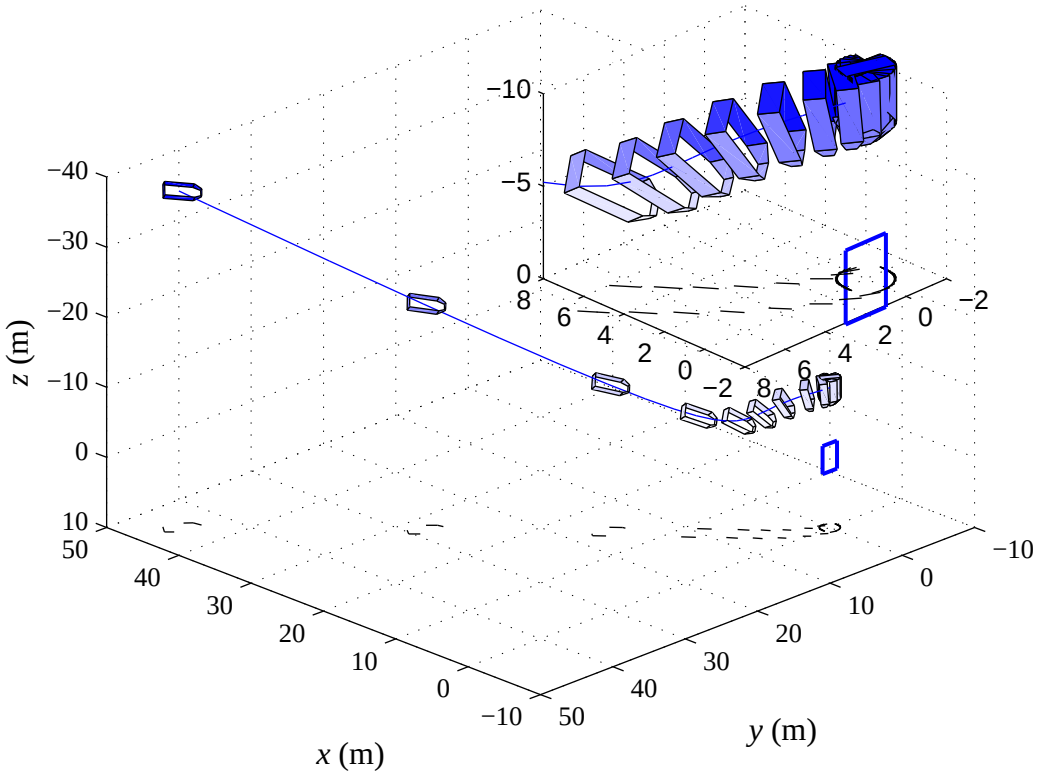

Figure 5a (color)

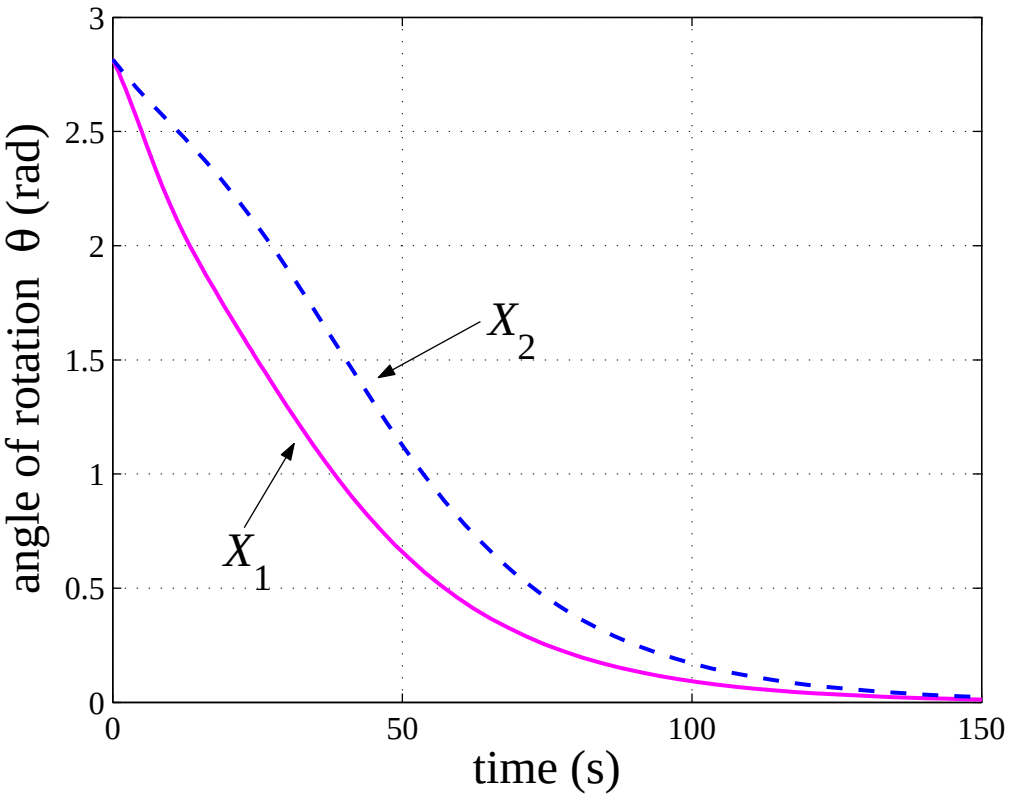

Figure 5b (color)

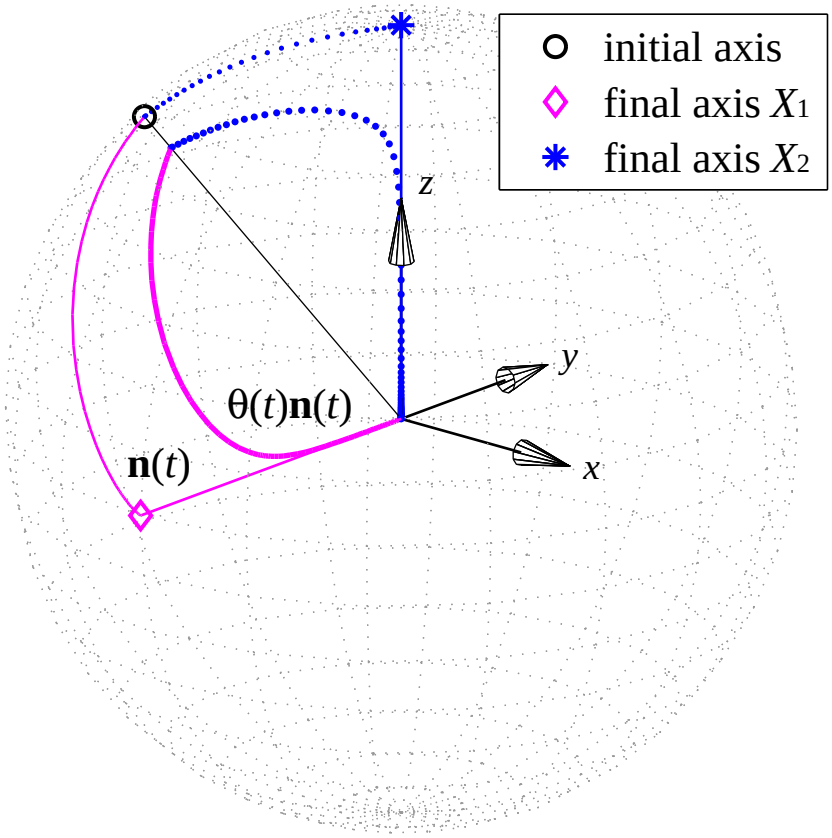

Figure 6a (color)

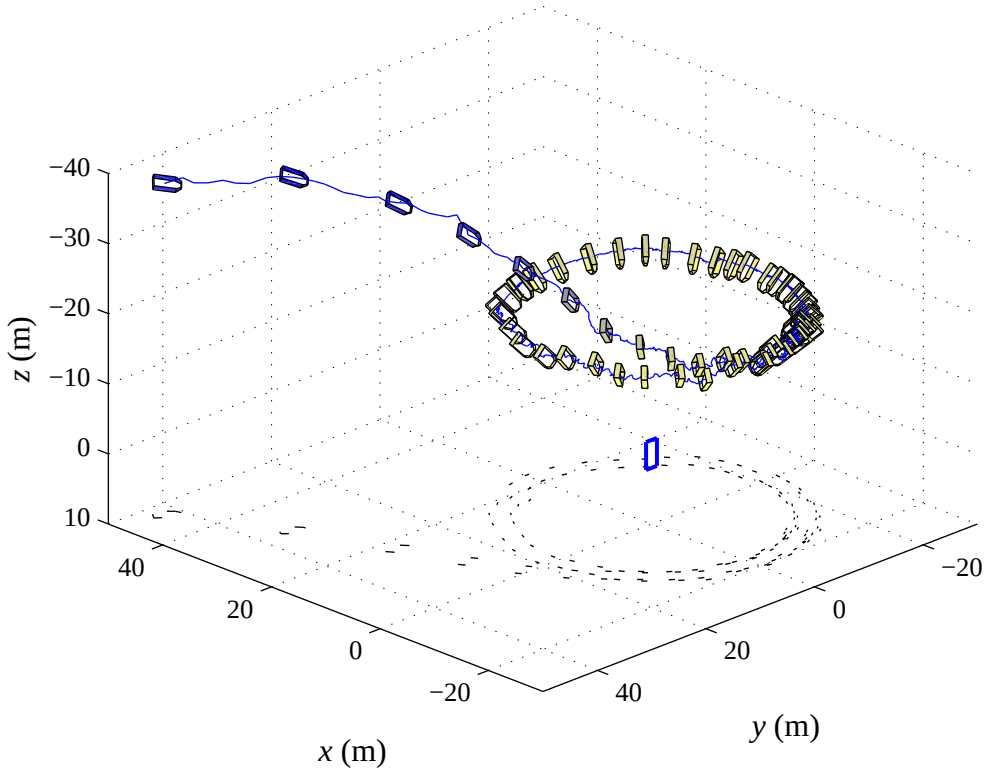

Figure 6b (color)

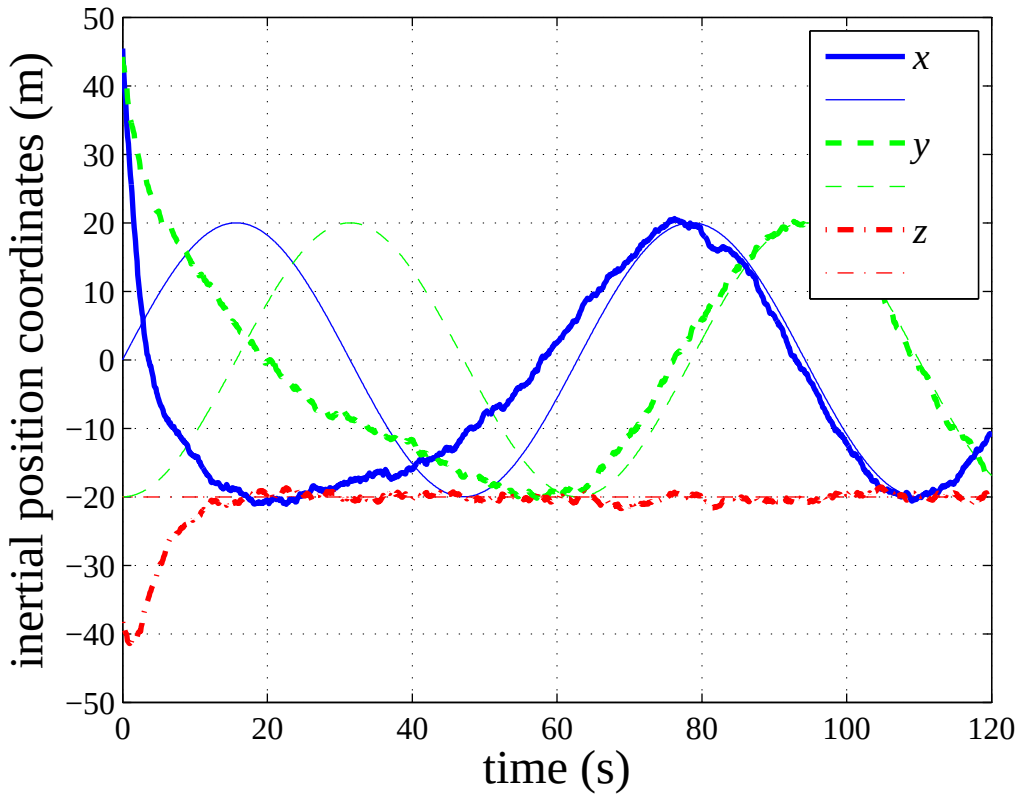

Figure 7a (color)

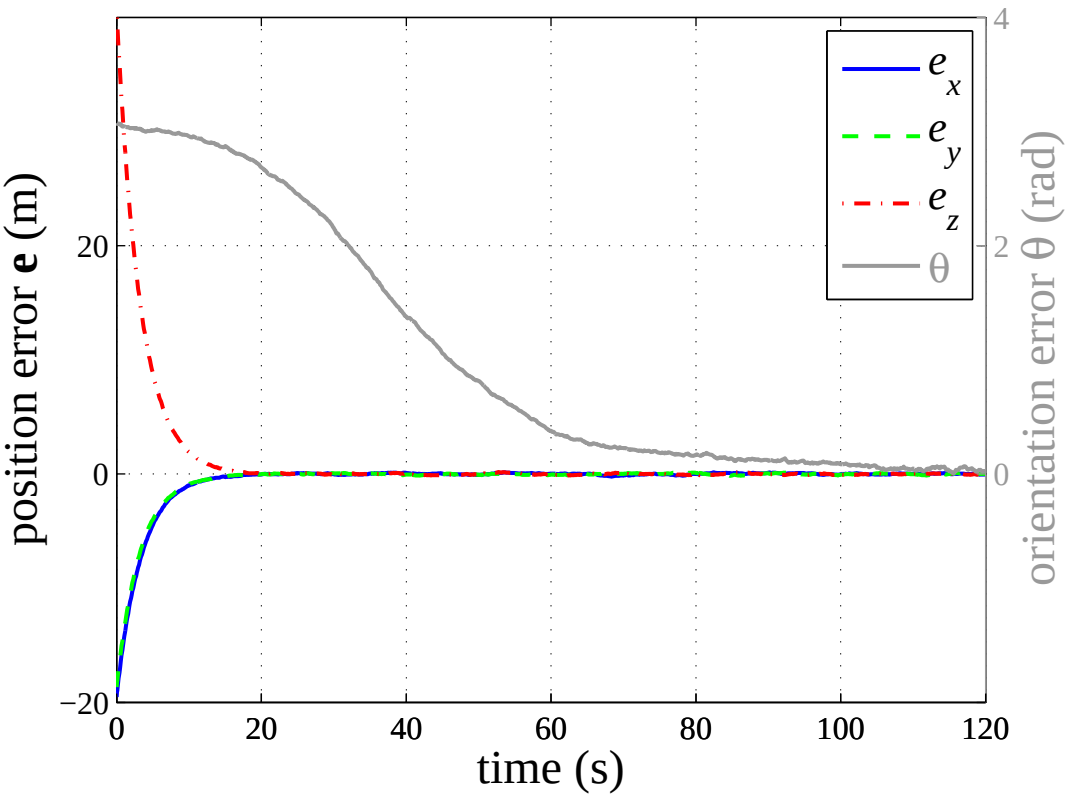

Figure 7b (color)